SIMULTANEOUS AMPLIFICATION OF MULTIPLE DNA TARGETS WITH OPTIMIZED ANNEALING TEMPERATURES

A Thesis
Presented to
The Academic Faculty

by

Nikita Pak

In Partial Fulfillment
of the Requirements for the Degree
Master of Science in the
School of Mechanical Engineering

Georgia Institute of Technology
August 2012

SIMULTANEOUS AMPLIFICATION OF MULTIPLE DNA TARGETS WITH OPTIMIZED ANNEALING TEMPERATURES

Approved by:

Professor Craig Forest, Advisor
School of Mechanical Engineering
Georgia Institute of Technology

Professor Todd Sulchek
School of Mechanical Engineering
Georgia Institute of Technology

Professor Baratunde Cola
School of Mechanical Engineering
Georgia Institute of Technology

Date Approved: 29 July 2012

ACKNOWLEDGEMENTS

I would first like to thank my advisor, Prof. Craig Forest, for his support, motivation, and guidance in both my research and person life. Your enthusiasm has been infectious, even if you have yet to see me have any sort of emotion. I would also like to thank the other members of my committee, Dr. Todd Sulchek and Dr. Baratunde Cola for being on my committee, and giving me feedback on my project. I would also like to thank everybody from the Precision Biosystems Laboratory, both current and past members. Specifically, I would like to thank Curtis for helping with my experiments and sharing his knowledge of PCR with me. I would like to thank Greg for coming up with the initial concept of the pressurized chip, and Nick for helping to manufacture chips for me. I would like to thank Mel for her general advice in both the lab and real world environment. Thanks especially to Chris for not only mentoring me as an undergraduate, but for countless hours of assistance in the shop, helping to run experiments, and for his incredibly helpful demenour both in the lab and on a personal level. Lastly, I would like to thank my mother, father, and Amanda for always believing in me and giving me support.

TABLE OF CONTENTS

LIST OF TABLES

LIST OF FIGURES

SUMMARY

The polymerase chain reaction (PCR) is an extremely powerful tool for viral detection and screening because it can detect specific infectious agents with great sensitivity and specificity. It works by exponentially amplifying a target viral DNA sequence to high enough concentrations through the use of specific reagents and thermal cycling. It has surpassed culture based methods as the gold standard for viral detection because of the increased speed and sensitivity. Microfluidic approaches to PCR have focused on decreasing the time to thermally cycle, the volumes used for reactions, and they have also added upstream and downstream processes that are of benefit for on-chip viral detection. While these improvements have made great strides over commercially available products in terms of speed, cost, and integration, a major limitation that has yet to be explored is the throughput associated with running PCR. Since each PCR reaction relies on primers with a unique annealing temperature to detect specific viral DNA, only a single virus can be screened for at a time. The device presented here uses two infrared laser diodes that are driven identically by the same laser driver to independently thermally cycle two chambers on the same microfluidic chip. Different temperatures are achieved in the two chambers by modulating the radiation reaching one of those chambers with an optical shutter. Closed loop temperature feedback in both chambers is done with a Labview program and thermocouples embedded in the polymer chip. This allows for accurate temperature measurement without inhibiting the reaction. To demonstrate the capabilities of this device, two different reactions were simultaneously amplified successfully on the same device that have annealing temperatures that differ by 15°C.

CHAPTER I

INTRODUCTION

The polymerase chain reaction (PCR) is a biochemical technique pioneered by Kary Mullis used to exponentially amplify as little as a single copy of DNA for genetic diagnosis [1]. Amplification of DNA is important in applications such as virus detection because not enough of the viral DNA is present in the sample to be able to determine which virus it is. The blood or saliva sample taken from a patient contains not only the genome of the virus, but also the patients own genome. It is therefore necessary to amplify a specific viral sequence of DNA that is not found in the human genome to high enough concentrations to be able to detect the signal from the background noise. PCR allows for the detection of viruses by amplifying a specific target sequence so that it can then be detected from the non-viral human DNA found in the sample. To determine which virus is present in the sample, specific primers for each virus are created that amplify a sequence only found on that virus. If the amplification is successful, then the known length of that DNA sequence will show up after running the PCR product through electrophoresis, a technique that separates DNA by length.

Before the advent of PCR, growing a culture from the patients sample was the standard technique for the detection of infectious diseases [2]. Culture methods require taking the patients sample and allowing the infectious agent to grow in a controlled environment. For viral detection, the healthy cells are inoculated with the sample and monitored for cytopathic effects every couple of days. This process takes between 2-10 days and has been shown to be less sensitive than PCR in clinical trials [2]. Bacterial culture is performed by a similar means, except a growth medium is supplied for the bacteria to flourish in. This process takes between 1-3 days and has

also been shown to be less sensitive than PCR [3].

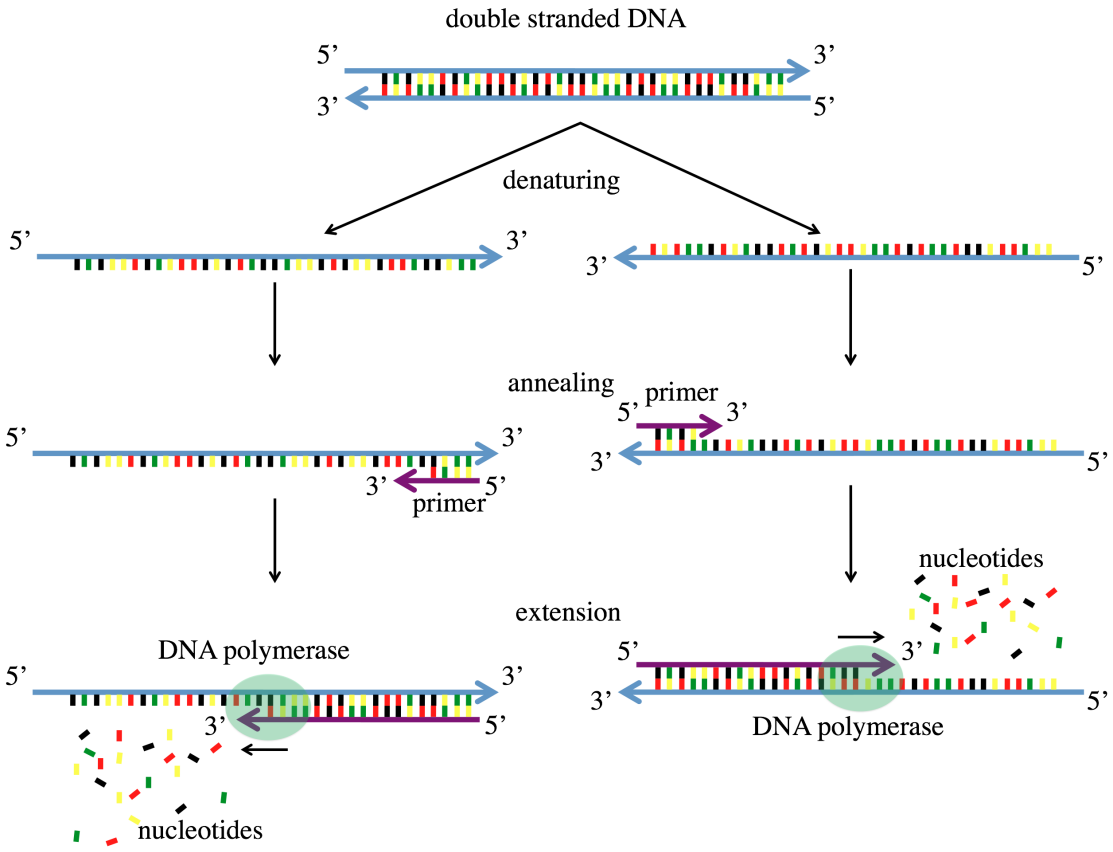

Figure 1: Representation of one cycle of PCR where a single piece of DNA is copied into two pieces. The double stranded DNA is first denatured into two single stranded pieces of DNA, then the forward and reverse primers are annealed to the 3' end of each piece of DNA, and finally the DNA polymerase extends the short primer the entire length of the DNA by adding complimentary nucleotides found in solution.

PCR relies on thermally cycling a mixture of ingredients, which consist primarily of the following: DNA sample, primers, PCR buffer, $MgCl_2$, nucleotides, and a heat stable DNA polymerase. The DNA sample is the purified DNA that has been taken from the patient for diagnosis. The primers are short strands of DNA fragments that have a specific sequence to amplify the DNA target being screened. A forward and reverse primer are both needed because the two single strands of DNA have different sequences at their 3' ends, where the primers attach. The PCR buffer is used to

mediate the pH of the solution while the $MgCl_2$ helps the polymerase function and also stabilizes the two strands of DNA. Nucleotides are the free DNA bases that are used in this process to create the new DNA sequences by attaching complimentary bases to the single stranded DNA. Finally, the heat stable polymerase is required to actually assemble the new DNA sequence on a single strand of DNA. It must be heat stable so that the polymerase itself does not denature in the high temperatures required for PCR.

There are three distinct temperature stages necessary to perform PCR: denaturing, annealing, and extension. In the denaturing step, the double stranded DNA is heated to 94°C to break apart the hydrogen bonds to form two individual strands of DNA. Next, the temperature is lowered for the annealing stage where the primers bond to the single stranded DNA. The exact temperature for this stage depends on the primers used, and is unique for each PCR reaction [4]. The temperature depends on the base pair content of the primers as well as their length. Finally, in the extension stage, the polymerase extends the primers by matching the complementary nucleotides that are in the solution to the DNA bases on the singe strands of DNA. In this way, a single piece of DNA is doubled every cycle of PCR. A representation of a single cycle of PCR is shown in Figure 1. This process continues until the thermal cycling is complete, or until one of the reagents is used to completion.

Typically, the thermal cycling required for PCR is done by a Peltier based device. These systems use a Peltier junction to heat and cool a metal block that holds tubes full of PCR solution. The typical volumes run in each tube are between 10-100 μL, and the devices can hold somewhere around 100 tubes. A temperature measurement device is embedded in the metal block for feedback control. The heating and cooling times vary based on the volume of solution put in the tubes, but overall run times are on the order of 2-3 hours. These relatively slow heating and cooling rates can lead to non-specific PCR products because of the long transition times between distinct

steps. This can lead to primer dimer formation, and decrease the overall efficiency of the reaction [5]. Other commercial approaches to thermal cycling such as the Roche Lightcycler [6] and Qiagen Rotor Gene Q rely on convective heating and cooling for increased cycling times while also decreasing the reaction volume to as low as 5 μL. They also have the ability to perform real time PCR, a type of PCR that uses fluorescence detection to quantify the number of DNA copies as thermal cycling is taking place [7]. While PCR is a very common technique these days with many positive attributes, there is still much room for improvement. Microfluidic approaches to PCR strive to eliminate the problems of cost, time limitations, and integration that are present with commercially available thermal cyclers. Cost can be reduced because the smaller reaction volumes used with microfluidics inherently reduce the use of expensive reagents, such as the DNA polymerase, which alone costs roughly $40 per microliter. The time to run PCR is reduced because smaller volumes heat and cool faster, which can also help with specificity because the transition times between PCR steps is reduced [8]. Finally, integration with upstream and downstream processes is the ultimate goal of microfluidic totally automated systems. Some processes that would be beneficial to integrate with PCR are DNA purification [9, 10], and elecrophoresis [11, 12, 13, 14]. No commercial thermocyclers have the capability to integrate with other processes.

Microfluidic thermal cycling methods fall under two categories: stationary, and flow-through. Stationary thermal cycling systems are similar to commercial devices in that the sample volume remains fixed while an external heat source takes the sample through the necessary temperature points. Flow-through devices have three distinct temperature regions that are always at the same temperature [15]. The solution is thermally cycled by moving it through these distinct temperature zones. The advantage of flow-through systems is that they offer the potential to integrate with other processes because the solution can be flowed to other parts of the device

for these processes. An example of a flow-through microfluidic PCR device is shown in Figure 2.

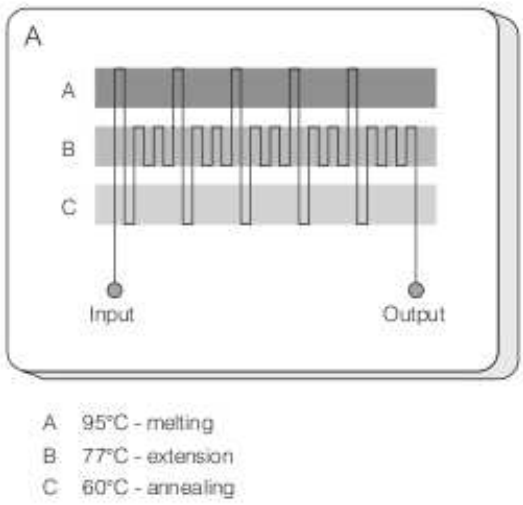

Figure 2: Schematic of a flow-through microfluidic PCR system where there are three distinct temperature zones that the reaction moves through to be thermally cycled [15].

Similar to commercially available products, conductive and convective heating sources have been used with microfluidic thermocyclers. Resistive heaters embedded on microfluidic chips [16], as well as devices that rely convection [17, 18] have been used in the past. Conduction based devices offer the advantages of faster heating rates and abilities to integrate with other systems; however, they consume a large amount of power and the heating device may interact with the solution. Natural convection based systems rely on the fluid flow caused by buoyant forces due to temperature gradients. These systems are advantageous because of the decreased complexity, due to the removal of parts such as pumps. They also require less power and can be very compact. However, the speed of these devices is based on the temperature gradient, which is a function of the primers used. Therefore, these systems may be better suited for some PCR reactions as opposed to others. Also, these systems require a relatively large sample volume (at least 10 μL). Forced convection systems are similar

to commercial products, but with increased speed due to the lower volumes. These suffer from the inability to closely pack together chips with different temperature conditions on the same device.

Microfluidic systems also introduce novel thermal cycling methods, the most important of which is radiative based heating. Within this category are several approaches ranging from broadband sources to focused radiation sources. Broadband sources, based on tungsten lamps, offer fast, non-contact heating of small volumes [19, 20, 21]. Both glass and polymer materials have been used for chips because the entire substrate and sample volume is heated uniformly. This technique has led to some of the fastest PCR ever performed (15 cycles in 240s) [22]. Radiative heating offers both a fast and non-contact means of thermal cycling, which is ideal for a disposable chip platform.

Laser-mediated infrared heating combines the advantages of speed and a non-contact heating source such as those found in broadband radiation with the advantages of a focused and monochromatic radiation source. Unlike the lamp based systems, laser based PCR systems only heat the solution and not the surrounding substrate which allows for even faster heating rates and the ability to focus the radiation over a very small volume. Others have been able to take utilize these advantages to perform PCR in droplets [23, 24, 25], that allow for very small sample volumes (15 pL) and rapid cycling times (200 s).

The major limitation of all the viral detection techniques presented here is the inability to screen for multiple different infectious agents simultaneously. Since each primer sequence used to amplify a specific sequence of DNA has a unique annealing temperature, it is impossible to thermally cycle different PCR reactions on the same device and get acceptable amplification. While it is possible to run the same device multiple times, this is extremely inefficient and costly. Multiplex and consensus

degenerate PCR are two variants that try to work around this limitation by simultaneously amplifying several different target sequences. Multiplex PCR is a technique that has multiple primer sequences within a single PCR reaction [26]. This allows for a greater amount of information to be obtained per run by targeting different sequences. The primers, annealing temperature, primer concentration, $MgCl_2$ concentration, and nucleotide concentration must be carefully chosen so that all sequences can amplify at a single annealing temperature [27]. This makes multiplex PCR a more difficult technique to master, and therefore less suitable for applications such as point of care clinical viral detection. Multiplex PCR is generally used in the analysis of deletions, mutations, and polymorphisms [27]. In consensus degenerate PCR, special primers allow for the discovery of new diseases based on conserved DNA sequences [28]. Primers with a consensus clamp that attaches to an evolutionary conserved sequence and a degenerate core that can attach to many different DNA sequences are specially developed for such applications. While this allows for the discovery of new sequences based on similarity to known sequences, it is not suited for the detection of multiple known sequences simultaneously.

PCR has replaced culture methods as the gold standard technique for detection of infectious diseases due to its much faster turnaround while still offering high sensitivity and specificity [2, 3]. Microfluidic approaches to PCR have further improved on the speed and cost associated with traditional PCR while also incorporating upstream and downstream processing. However, a current bottleneck of PCR that has yet to be addressed by any approach is the inability to screen for multiple infectious agents simultaneously due to the specific annealing temperature required for each reaction. The device presented here is an initial attempt at highlighting some of the benefits of laser mediated PCR. Specifically, the ability to rapidly cycling different reaction on the same device by taking advantage of the ability to guide and modulate a laser source with higher precision than other heating methods. A device will be

demonstrated that can simultaneously cycle any two reactions on the same device, regardless of their specific annealing temperatures.

CHAPTER II

MICROCHIP MATERIAL AND MANUFACTURING

2.1 Material Selection

The initial concept behind this project comes from Dr. James Landers work with a tungsten lamp based infrared thermocycler [19, 20, 21]. Their work typically relies on glass microchips with etched features. Initial attempts at using these glass chips with our lasers failed because sufficiently high temperatures could not be reached. This problem was investigated because one of the reasons for switching to a laser source was the known higher efficiency of heating water with a laser source as opposed to a blackbody source.

An effective medium model and finite element model were implemented and experimentally validated for radiative heating in glass and polymer microchips coupled to blackbody and monochromatic radiation sources. The glass device used was a two-chamber microchip designed for PCR with 500 nL samples, courtesy of James Landers at the University of Virginia. The device is made of borosilicate glass and was fabricated using standard photolithography, wet-etching, and thermal bonding techniques. The polymer device was made of poly (methyl methacrylate) (PMMA) and possesses geometry similar to that of the glass device. Unlike the directly milled chips that were eventually used with the laser system, it was fabricated by laser etching the features with a CO_2 laser cutter (VersaLASER, VLS3.50). The dimensions were confirmed with surface profilometry (Dektak 3030) and the enclosed two-layer device was thermally bonded in boiling water [29]. A 50 W tungsten-filament incandescent projector lamp (Eiko, CXL/CXR 8 V 50 W) was used for the blackbody source and a 600 mW 1450 nm laser diode (Hi-Tech Optoelectronics, LMD-1450-600-33) for the

monochromatic source, which was selected to match an absorption band of water. The experimental setup is depicted in Figure 3. For the lamp, the total power output is calculated from the electrical power supplied, P = V x I, where V is the voltage and I is the current. Spectral data for determining the absorbed radiation was transcribed from a spectral irradiance curve with a resolution of 25 nm for the range from 300 to 5000 nm. For the laser, the power output is a known function of the supply current and was confirmed with a power meter. The Gaussian beam profile of the laser diode was sampled with a spectral resolution of 0.5 nm for the short- wavelength infrared range of 1440-1460 nm.

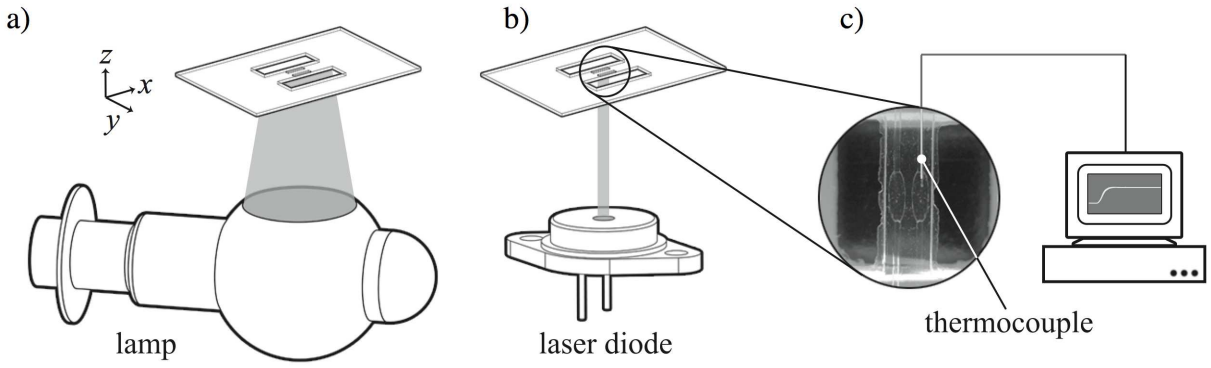

Figure 3: Experimental setup to measure heating in a glass chip heated with a tungsten lamp a), and a PMMA chip heated with an infrared laser b). Thermocouple insertion technique used for both experimental setups c).

Since the blackbody radiation of the lamp melts PMMA and therefore excludes this combination from practical testing, three cases were modeled and tested experimentally: (1) lamp heating of water in glass, (2) laser heating of water in glass, and (3) laser heating of water in polymer. Temperatures were kept between the ambient 25°C and 100°C to avoid damaging the PMMA microchip, which has a glass transition temperature of approximately 105°C, and because these are the operating temperature ranges of PCR. Therefore, the radiative sources were not always operated at full power.

2.1.1 Thermal Modeling

The effective medium and finite element approaches were implemented for each case. The thin substrates of most microfluidic devices results in negligible thermal gradients across the thickness (z), leaving convection as the primary mode of heat loss. On the other hand, thermal gradients across the width (y) and length (x) of a device may not be sufficiently uniform for the application of the effective medium assumption. As a preliminary assessment of this temperature uniformity, a three-dimensional finite difference model, programmed in computation software Engineering Equation Solver (EES), calculated the steady state temperatures for a set of nodes representing the heating cases for heating in a glass chip for the lamp and laser. The transient solutions for each case were first calculated by applying the effective medium assumption and were solved using a fourth and fifth order Runge-Kutta method in Matlab. The energy balance equation is applied as

$V\rho c_p \frac{dT}{dt} = Q_{rad,in} - Q_{cond,out} - Q_{conv,out} - Q_{rad,out}$,

where

$Q_{cond,out} = \frac{k_s A_{cond} \Delta T}{L}$,

$Q_{conv,out} = hA_{cond}\Delta T$,

and,

$Q_{rad,out} = FA_t\varepsilon_s\sigma(T_4 - T_{inf}^4)$

Here, T is the temperature, V is the total volume of the heated region, and material properties such as density, ρ, and specific heat at constant pressure, c_p, which apply to the entire "effective medium," are calculated with mass-weighted averages of the constituent liquid and solid properties. $Q_{cond,out}$ is the conduction losses to unheated parts of the microchip (if applicable), where k_s is the thermal conductivity of the substrate, A_{cond} is the cross-sectional area at the interface, and L is the length of the conducting region in the direction of conduction. $Q_{conv,out}$ is the free convection out, where A_{conv} is the total convecting surface area of the medium

and h is the heat transfer coefficient. This is calculated from the Nusselt number, which is found using an empirical correlation with the Rayleigh and Prandtl numbers based on the particular geometry of the convecting body. Q_{rad},out is the radiation out, where F is the shape factor, A_t is the total exposed area of the control volume, ε_s is the emissivity of the medium, and σ is the StefanBoltzmann constant.

The theoretical radiation into the control volume, $Q_{rad,in}$, is calculated from the optical properties of the source and the geometric and absorptive properties of the absorbing media. For the source, spectral irradiance data is scaled by integrating over its full spectrum and equating it to the known total power output. This yields the scaled spectral power distribution, $P_0(\lambda)$. The losses due to reflection at the air-glass and glass-water interfaces were calculated to be 4% and 0.5% respectively based on simplified reflection coefficient equations for near-normal incidence. Using absorption coefficients, $\alpha(\lambda)$, of the absorbing media and the path length, l, through which the radiation travels, the absorbed power $P_{abs}(\lambda)$ is given by the BeerLambert law as $P_{abs}(\lambda) = P_0(\lambda)(1 - 10^{-\alpha(\lambda)l})$. This is integrated with respect to wavelength and, in the case that the focal spot is larger than the control volume, adjusted for the incident area and, if necessary, the intensity distribution to provide the radiative power into the control volume. For the spatial and temporal scales in this study, the quasi-Gaussian distribution of the laser and the lamp focal spot were assumed uniform. $Q_{rad,in}$ is then the sum for all absorbing bodies that constitute the effective medium.

The preliminary tests of the appropriateness of the effective medium approach using finite difference analysis to calculate steady state temperatures is shown in Figure 4, which reveals the temperature profiles for lamp and laser heating in glass over the length, width, and thickness of the entire device. While heating with the blackbody source results in roughly uniform temperatures, the laser heating profiles show more localized heating behavior inconsistent with the prerequisite condition for

the effective medium assumption.

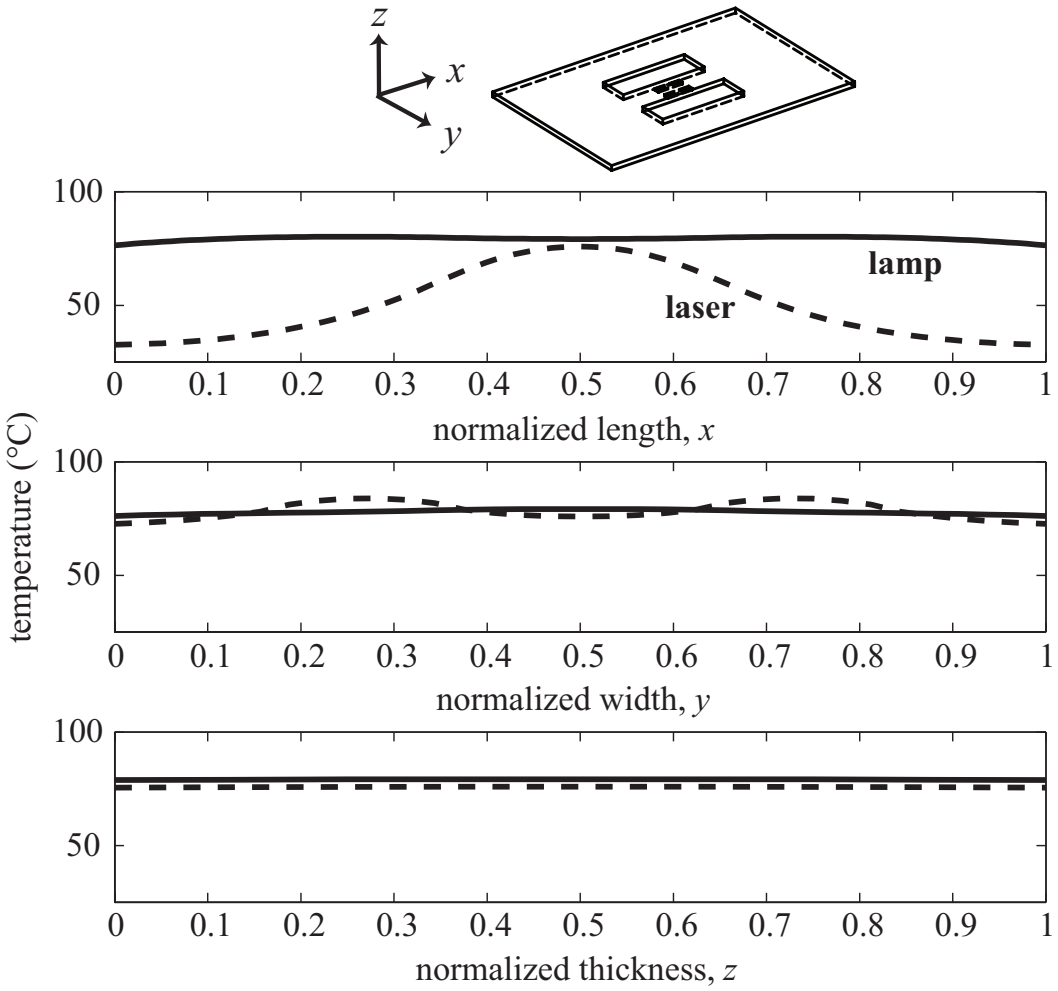

Figure 4: Laser and lamp temperature profiles in the x, y, and z directions. The laser heating profiles show localized heating as apposed to the uniform heating of the lamp profiles.

The reasons for this behavior are elucidated in Table 1, which summarizes the absorbed radiation values for the lamp and laser heating in the glass microchip. Despite the much greater efficiency of laser heating an aqueous sample, the lamps higher power output and significant absorption by the glass results in a device of uniform temperature and conductive losses from the chamber are therefore minimized. Conversely, the laser heating is localized in the liquid medium because of the smaller focal spot and the transparency of the microchip substrate to the infrared radiation.

Table 1: Percentage of total radiation absorbed by water and glass for a laser and lamp source.

Source		Absorbing Medium
	Water	Glass
Lamp	2%	10%
Laser	70%	1%

This results in greater heat sinking by the substrate, i.e., in-plane conductive heat loss.

Figure 5 shows a further examination of the absorbed spectral power from the lamp as absorbed by both water and glass. Although the glass is not quite as efficient in absorbing the blackbody radiation per unit area, it experiences a larger area of exposure to the lamp output and in turn absorbs much more power than the water. The equivalent data for the laser would appear as a near vertical line at 1450 nm for absorption by water and a negligible peak for glass absorption.

The cases were then solved using finite element software COMSOL Multiphysics. Simplified geometry of the glass and polymer microchips was created. The reaction chambers were specified as water volumes and were assigned heat generation values based on the theoretical absorbed radiation. For the case of the lamp heating in a glass microchip, the glass and water were both assigned heat generation values. For the laser heating in glass and polymer chips, only heat generation in the liquid reaction chambers needed to be specified since the absorption of the 1450 nm laser output by the solid substrates is negligible. The finite element solver was run for a time domain of 60 s and temperature values were recorded every 0.01 s at 10 equally spaced points along the centerline of the reaction chamber. The values at the 10 points were then averaged to obtain the mean temperature for the liquid chamber. A mesh sensitivity test revealed no need for refinement of the auto-generated mesh.

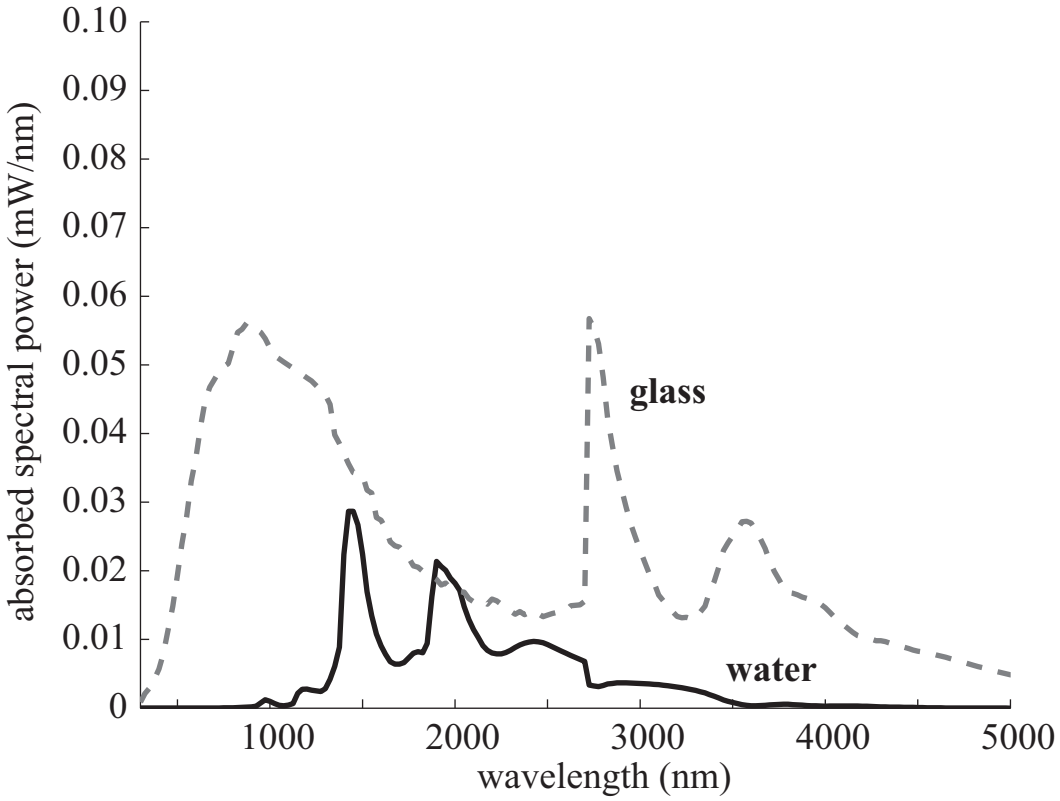

Figure 5: Tungesten lamp radiation absorbed by water and glass. The lamp is better able to heat a solution in a glass chip because both the water and the glass substrate absorb the blackbody radiation

2.1.2 Experimental Validation

For experimental validation of the effective medium and finite element modeling, lamp heating was performed at an intermediate power level of 9.3 W as specified in the models. Laser heating in glass was performed at the full power of 620 mW. For heating in the polymer device, the power was reduced to 300 mW to prevent the heated water from causing channel deformation due to thermal expansion and material softening above the glass transition temperature. The lamp was powered with a variable power source and focusing was achieved with an ellipsoidal retroreflector, which provided a roughly circular focal spot with a diameter of about 10 mm. The laser was driven with a low-noise current source (Thorlabs, ITC133) and controlled with a 10 Hz pulse

width modulated signal output from a Labview program. The diverging beam was collimated with an aspheric molded glass lens (Thorlabs, A230TM-C), producing a roughly 5 mm by 2 mm elliptical spot. The inherent ramping of output intensity of each source was measured using an optical power meter (Thorlabs, PM10-3) and rise times were considered negligible compared to the transient heating time scales. Temperature was measured using a T-type thermocouple (Physitemp Instruments, T-240C). Measurements were recorded with Labview and data collection was synchronized with the power supplies for the lamp and laser using a digital output from the DAQ. The thermocouple, which has a 0.003" diameter and response time of 34 ms, was inserted into the reaction chamber through an inlet channel, as pictured in Figure 3. The thermocouple tip was positioned with minimal protrusion into the chamber to avoid direct irradiation. With an insertion length of 0.5 mm and a diameter of 0.06 mm, the thermocouple occupied only 0.5% of the total chamber volume and had a negligible influence on the thermal mass. The optical characteristics for the various heating cases and the results of the uniformity testing suggested the use of finite element methods to capture the localized heating by the laser. The transient models are compared to experimental data in Figures 6-8. As a metric for the accuracy of the models when compared to the experimental data, root mean square deviation was calculated as $\sqrt{(1/n)\sum |T_{exp} - T_{model}|^2}$. For lamp heating of glass, shown in Figure 6, the effective medium model exhibits a deviation of 4.54°C while the finite element model matches slightly better with a deviation of 3.10°C. For laser heating in glass, the effective medium model deviates considerably with a mean difference of 61.17°C, which is to be expected from the temperature uniformity results of Figure 5. The finite element model offers a much better correlation with a deviation of 1.37° C. Similarly, for laser heating in the polymer device, the effective medium model is 59.25°C off while the finite element model deviates by an average of 3.14°C.

With the lamp powered at 9.3 W, which corresponds to the data in Figure 6,

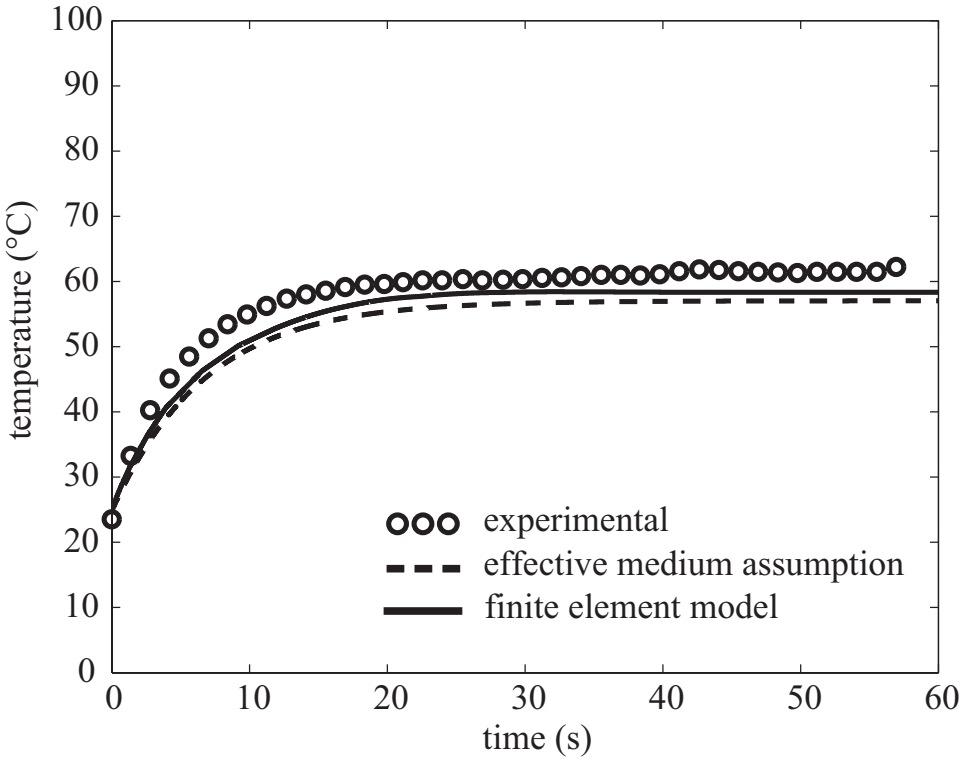

Figure 6: Tungsten lamp heating of a glass microchip.

the radiation absorbed by the water is approximately 20 mW while the glass absorbs 110 mW and results in a steady state temperature of 62°C. To compare, the laser operating at its full power of 620 mW imparts 435 mW to the water but the sample only reaches a steady state temperature of 64°C as shown in Figure 7. Without a heated substrate, the liquid volume suffers from significant conductive losses and the ratio of steady state temperature to power absorbed by the water is much lower than that for lamp heating. The less thermally conductive PMMA microchip exhibits reduced conductive heat loss, and with the laser power at less than half of that used for glass chip heating, the steady state temperature is a much higher 95°C as shown in Figure 8. Small discrepancies between the modeled thermal responses and the experimental data can be attributed to the difficulty in achieving the perfect alignment and spacing inherent in the modeled cases. Additionally, the adjustments made for the theoretical intensity distribution of the sources will be approximations

of the actual distributions.

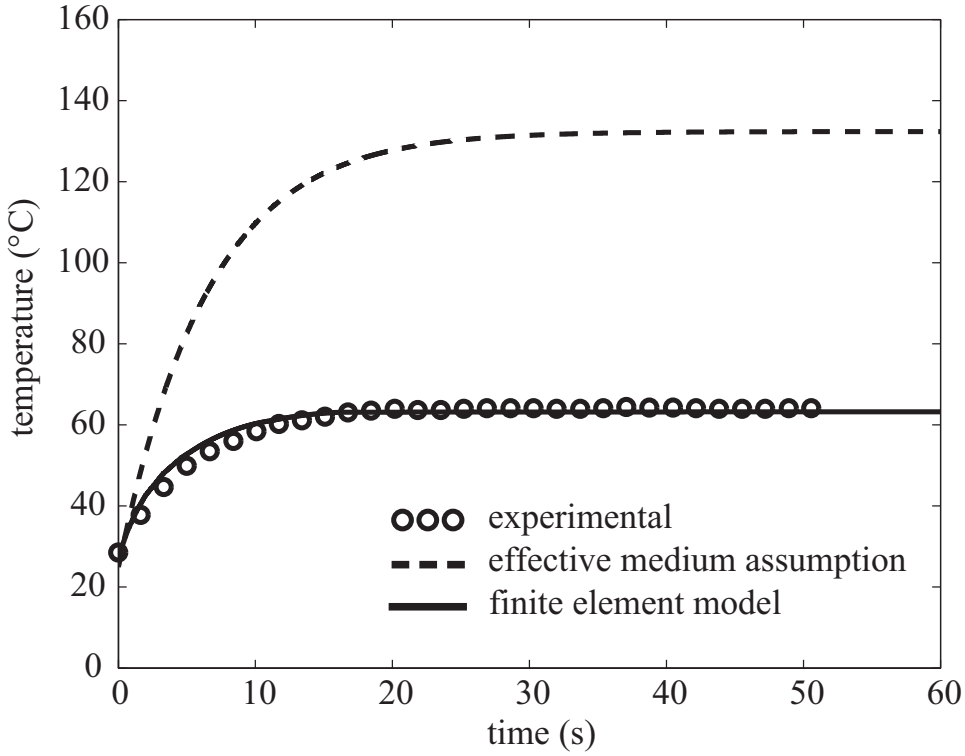

Figure 7: Laser heating of a glass microchip showing the inability of the effective medium assumption to capture the localized heating properties of the laser.

This data showed that while a laser is much more efficient at heating the aqueous solution inside the reaction chambers, the correct material must be chosen for the chip substrate to take advantage of this property. A polymer chip needs to be used for laser-based thermocycling because traditional glass microchips act like heat sinks and remove the heat from the solution through conduction in the x-y plane.

2.2 Chip Manufacturing Technique

After it was determined that polymer chips were necessary for laser-based thermocycling, many fabrication techniques including injection molding, hot embossing, and laser cutting were attempted for chip manufacturing. Injection molding is a great manufacturing technique for polymers because it is extremely cheap and fast after

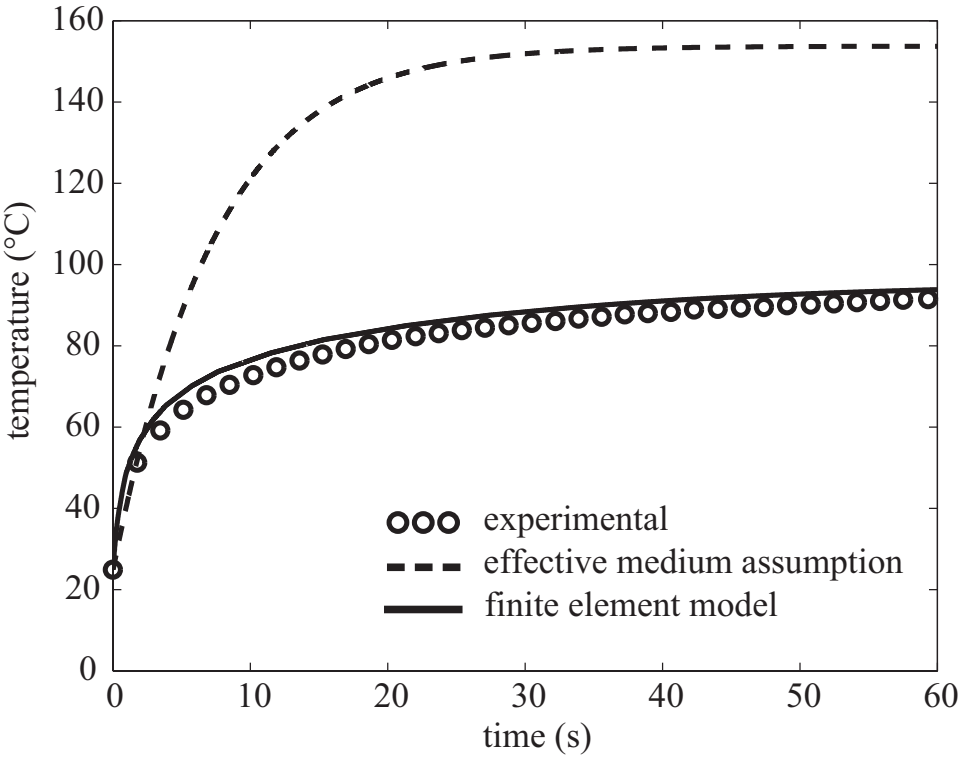

Figure 8: Laser heating of a PMMA microchip. Since the PMMA substrate is less conductive than the glass, the steady state temperature of the solution is able to be much greater.

the initial mold is created. This was the first approach attempted because of these advantages. However, in a research setting, the time to make and subsequently modify the molds is a hindrance while developing the correct chip geometry. Hot embossing was attempted next, but the large aspect ratio of chamber depth to chamber width used in our devices often led to inconsistent features being molded. Laser cutting works by cutting thin layers of various materials, stacking them together, and thermally bonding them. This technique is fast and allows for quick modifications of chip designs, but the disadvantage with this approach is that for chips such as the ones used on this project, the fairly large z dimensions requires many layers to be cut and bonded. This leads to difficulties bonding, especially at the edges of the laser cut holes. It was determined that direct machining of the polymer substrate was

the best method for this device because it is fast, inexpensive at high volumes, and extremely repeatable. Also, it is much easier to make revisions to chip designs with this technique as opposed to something like injection molding.

2.2.1 Direct Polymer Micromilling

Microchips are fabricated from 1.5 mm thick PMMA at a rate of two chips per minute, using a 3-axis vertical milling center (Haas, OM-1A) capable of accurate positioning within 10 μm and repeatability of 6 μm. The spindle operates at speeds up to 30,000 rpm, enabling the use of miniature end mills and drill bits with sub-millimeter diameters. Tools are zeroed to the polymer workpiece by detecting electrical conductivity between the tool tip and the base of an aluminum fixture [30] that was milled and used to align and rigidly hold the polymer workpiece, since small part deflections can easily damage the fragile tooling.

A corner relief was pocketed into the fixture along with features for interfacing with a standard vise to allow repeatable positioning. Strap clamps were laser cut from 3.175 mm acrylic, which was chosen to avoid marring the surface of the workpiece. These were configured in a third-class lever arrangement and the screws were hand-tightened to provide clamping force sufficient to overcome cutting forces. Toolpaths were manually written in G-code to achieve the relatively simple designs but can also be programmed using computer-aided manufacturing (CAM) software for complex geometries. A photograph of the milling process can be seen in Figure 9. Coolant is used during the milling process, and this must be cleaned off with isopropyl alcohol and deionized water before using the chips.

After milling and cleaning the chips, another blank piece of 1.5 mm PMMA is thermally bonded to the bottom of the chips to seal them. Thermal bonding is done on the custom brass thermal press seen in Figure 10. The press is put on a hotplate set for 170°C for 45 minutes, and a torque screwdriver is used to tighten the bolts of

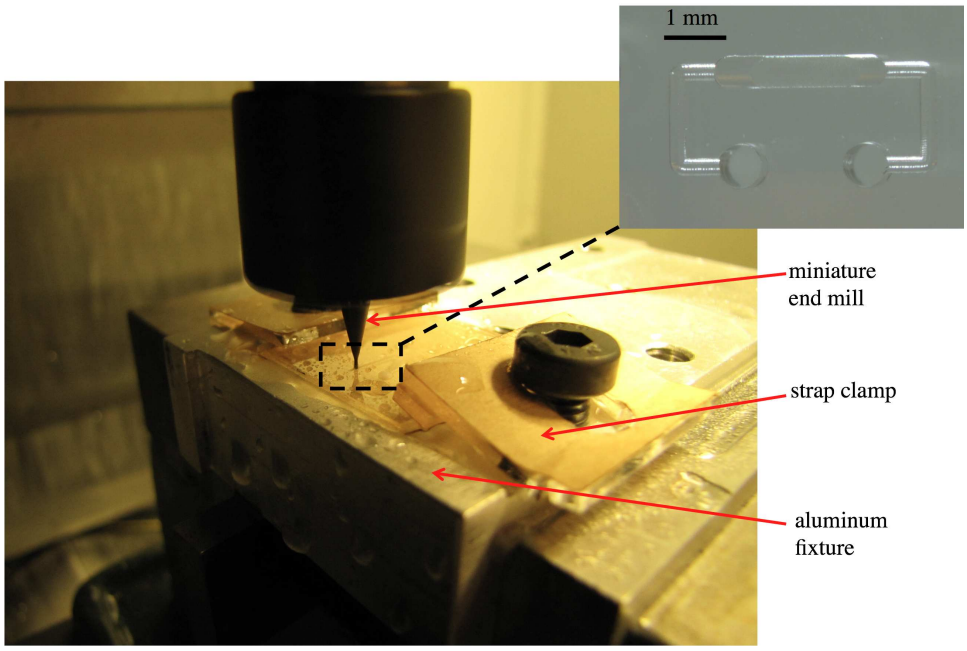

Figure 9: Photograph of direct milling of PMMA substrate in chip manufacturing process. The aluminum fixture is used to zero the chip in the x-y plane, and the end mill in the z direction. The inset shows a typical milled geometry.

the press to 0.339 Nm (48 in-oz). After 15 minutes and 30 minutes of bonding, the bolts are re-tightened to the same specification. This is done because as the chips heat up the thermal expansion in the bolts as well as the deformation of the PMMA pieces leads to loosening of the bolts. After 45 minutes, a timer automatically turns off the hotplate and the chip is allowed to cool for an additional hour before it is cleaned and used.

Altering a design and making a new batch of microchips can be easily accomplished in less than one day with these milling and thermally bonding processes. Materials such as PMMA, polycarbonate, and a biocompatible grade of cyclic olefin copolymer (COC) have all been successfully used for a substrate. PMMA was chosen because it is most quickly machinable, while retaining excellent optical, thermal, and biocompatible properties [31]. Another advantage is the three-dimensional geometries attainable with micro-milling in order to create path lengths amenable to maximum

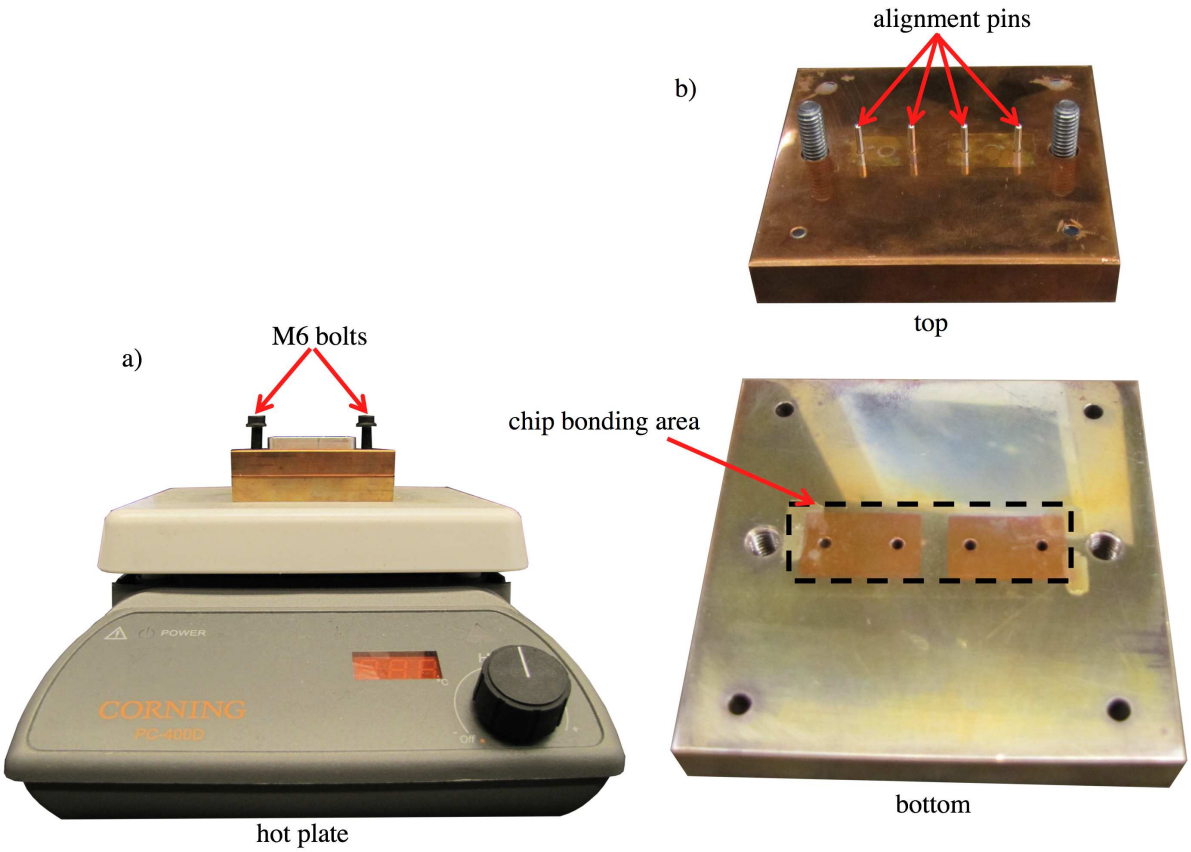

Figure 10: Thermal bonding technique using hotplate and torque screwdriver tightened M6 bolts on a copper press. Alignment pins are used in this process so the alignment holes on the chips do not move with respect to each other as the polymer is deformed through the bonding process.

absorption as well as control of the surface-area-to-volume ratio for optimum heat transfer characteristics and minimal adsorption of biological reagents to the interior microchip surfaces.

CHAPTER III

SYSTEM

A major problem with both commercial and microfluidic based approaches to PCR is the throughput. While commercial convective based approaches and all of the aforementioned microfluidic systems have been able to decrease the time required for thermal cycling, a major time limiting problem is the necessity to have unique temperature profiles for different PCR reactions. Since each primer has a unique annealing temperature for which it binds to the single stranded DNA, it is necessary to have an optimized annealing temperature for every reaction [4]. Commercially available gradient thermocyclers can do a range of annealing temperatures of up to 30°C during each run. However, not only do these have the same problems of large volumes and slow cycling times associated with other Peltier based products, these are not the best for fine tuning an exact annealing temperature for each reaction. The gradient gives a range of temperature values in the thermocycler, but it does not specify an exact temperature for each sample. Therefore, to truly use the optimized annealing temperature for each reaction, each reaction must be run at each gradient temperature. This is extremely costly and does not solve the problem of increasing throughput for each run. Gradient thermocyclers are really just a means of finding the optimum annealing temperature for a specific reaction experimentally.

A system that is capable of performing multiple different reactions on the same device simultaneously would greatly increase the throughput of running PCR. This would be a huge benefit in applications such as a viral outbreak or point of care screening. In cases like this, where the virus is not known, the ability to screen one sample for multiple DNA targets simultaneously would be a huge advantage over the

current approach, and would lead to faster treatment.

3.1 Dual Independent Temperature

The system developed allows for different reactions to be run in each chamber of the same chip by modulating the radiation reaching individual chambers. Unlike other radiation sources, such as a tungsten lamp, laser radiation is focused. This property allows for the ability to direct the radiation exactly over a single chamber for greater individual temperature control. Previously, it was shown that only the solution, and not the substrate, is heated with a laser source. Taking advantage of this property allows for reaction chambers to be closely packed on the same chip and still be thermally independent. In this system, a single laser driver is used to control two identical 1450 nm laser diodes. Since the diodes are connected in series, they are both driven identically. The laser power as a function of driving voltage for a single laser and both lasers in series is shown in Figure 11. In order to provide individual control to each chamber, one of the laser diodes is modulated with an optical shutter to attenuate the radiation reaching that chamber. Initially, an attempt was made at using a single laser diode and lens array to split the beam into two equal sources as opposed to two individual laser diodes. Unfortunately, it was not possible to find a commercially available 1450 nm laser diode with enough power to reach the denaturing temperature of 94°C in two chambers.

The shutter, as seen in Figure 12, is a miniature solenoid with a piece of foil attached at the end to block the infrared radiation. It is driven at 10 Hz, and has a travel distance of 8.9 mm. It works by decreasing the radiation reaching the chamber, and therefore decreasing the temperature of the solution in that chamber. The shutter is driven by a 10 Hz pulse width modulated square wave from the Labview program. The USB-6221 BNC data acquisition board (DAQ) used for this project has eight clocked digital input/output pins. One of these outputs is used to send the pulse

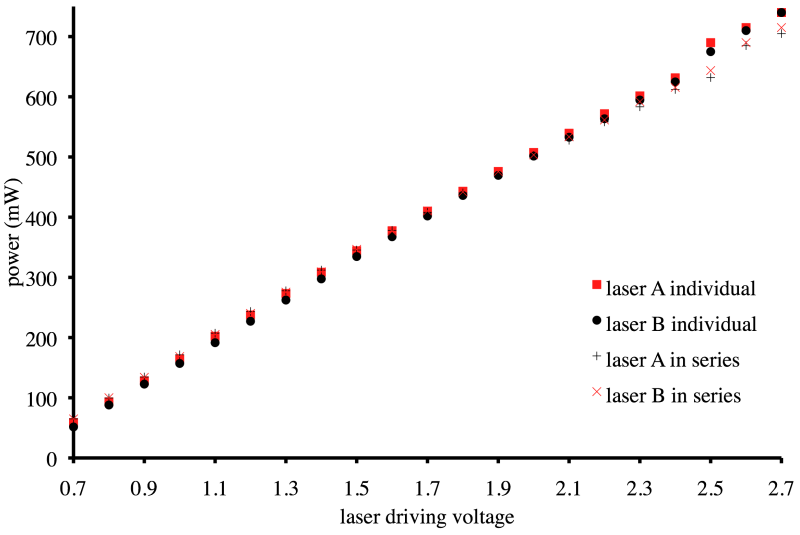

Figure 11: Laser power of both 1450 nm laser diodes when each is connected individually to the laser driver, and when both are connected in series to the same laser driver.

width modulated square wave to the solenoid because the hardware timing of these outputs ensures an extremely accurate signal. Other methods for reproducing square waves in Labview depend on software timing, which will vary with the amount of programs being run on the computer.

In order to vary the amount of radiation reaching the chamber through the shutter, the duty cycle of the square wave is changed. The duty cycle is the percentage of time the high portion of the square wave is sent. A plot of the normalized laser power as a function of shutter duty cycle at 10 Hz is shown in Figure 13. This shows that the relationship between the transmitted power that reaches the reaction chamber and the duty cycle that drives the shutter is linear.

To show the effects of modulation on the solution temperature inside of the microchip, two experiments were performed. First, it was important to understand the maximum temperature difference achievable between adjacent reaction chambers on

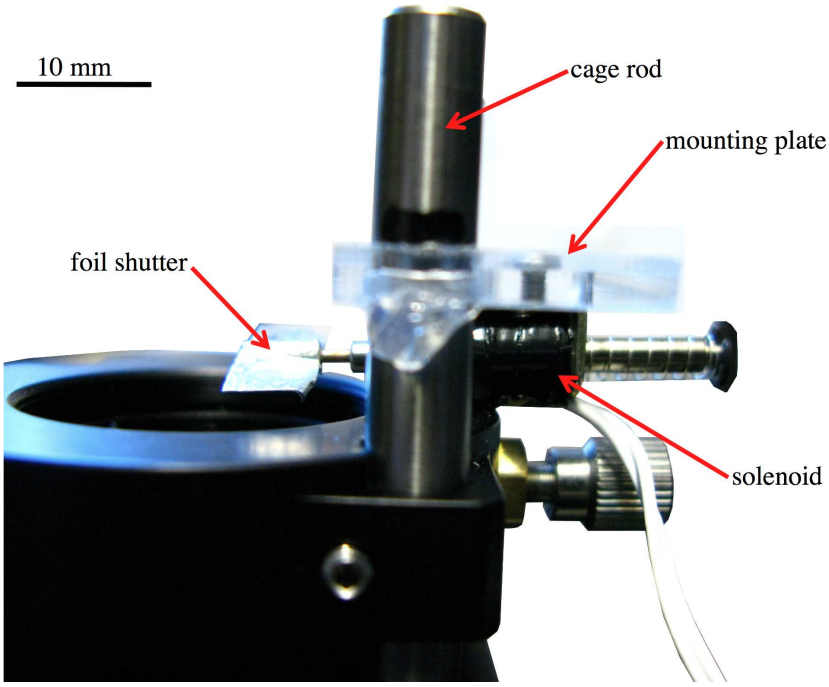

Figure 12: Mechanical shutter based on miniature solenoid used to attenuate the radiation reaching one chamber. The solenoid is mounted on a PMMA plate that is affixed to the cage rod system with an adhesive.

the same chip. A PMMA chip was made with 1 μL chambers positioned 1mm apart. This geometry was entered into the COMSOL model previously described with the same conditions as before. One chamber of the chip was given 10 different volumetric heat generation values to simulate heating by the laser, while the other was not heated at all, except for the conduction from the heated chamber. Both chambers were allowed to reach steady state and the temperature inside the chambers was taken as an average of 10 points per chamber. Next, this was done experimentally by driving the laser at 11 different powers and measuring the temperature inside each chamber with a thermocouple while the shutter was given a duty cycle of 1. This means that the shutter was completely blocking the laser from reaching that chamber. The steady state temperature of the irradiated chamber is plotted against the temperature difference between the two chambers for both the experimental results and the theoretical results from the COMSOL model in Figure 14. These results show that for a chip

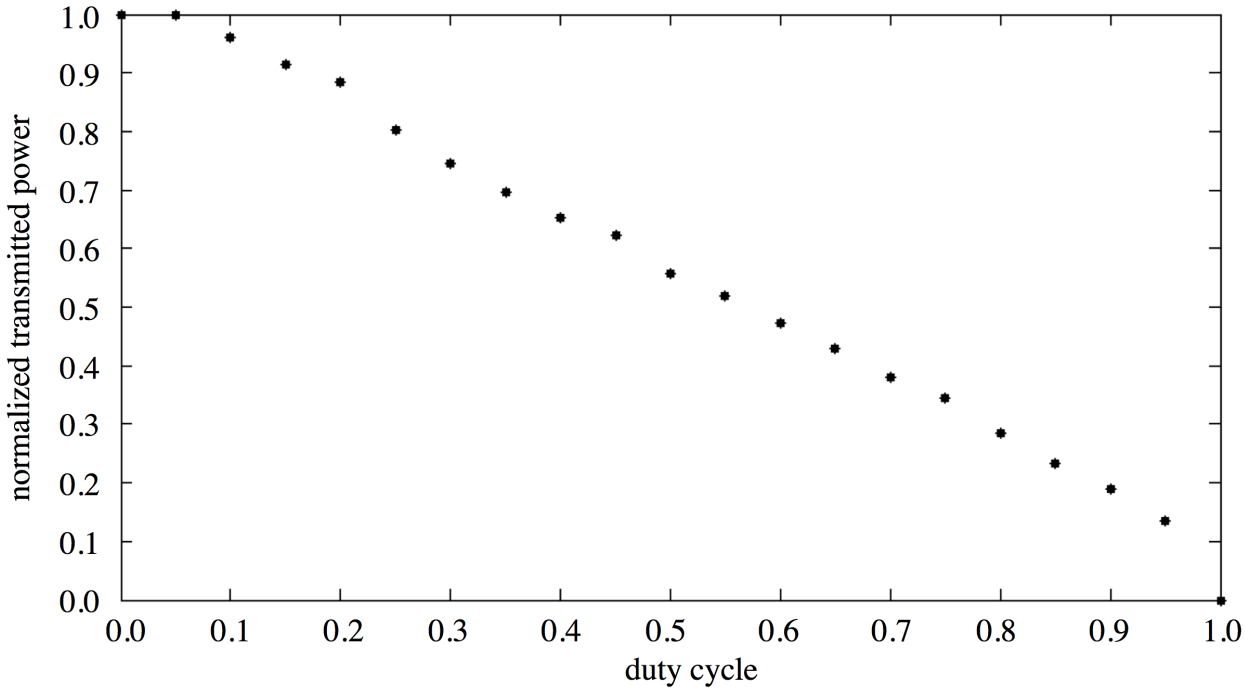

Figure 13: Normalized power reaching the reaction chamber as a function of shutter duty cycle.

with 1 mm spacing of 1 μL reaction chambers, the maximum temperature difference at temperatures relevant to PCR (50°C-70°C for annealing temperatures) is about 6°C-10°C. Even for such close packing of chambers, this is a large enough range to successfully perform PCR with many different primers.

The second test that was performed shows the ability of the shutter to hold a steady state temperature with minimal deviation, and also to be able to achieve different steady state temperatures by changing the duty cycle. To show this, the same chip was used with two 1 μL chambers spaced 1 mm apart. Thermocouples were inserted in both chambers to measure the temperature. A Labview program was used to maintain the temperature of one chamber at around 50°C while the other chamber's temperature was decreased by varying the duty cycle of the shutter. The results are shown in Figure 15. The shutter was operated at 10 Hz, and the duty

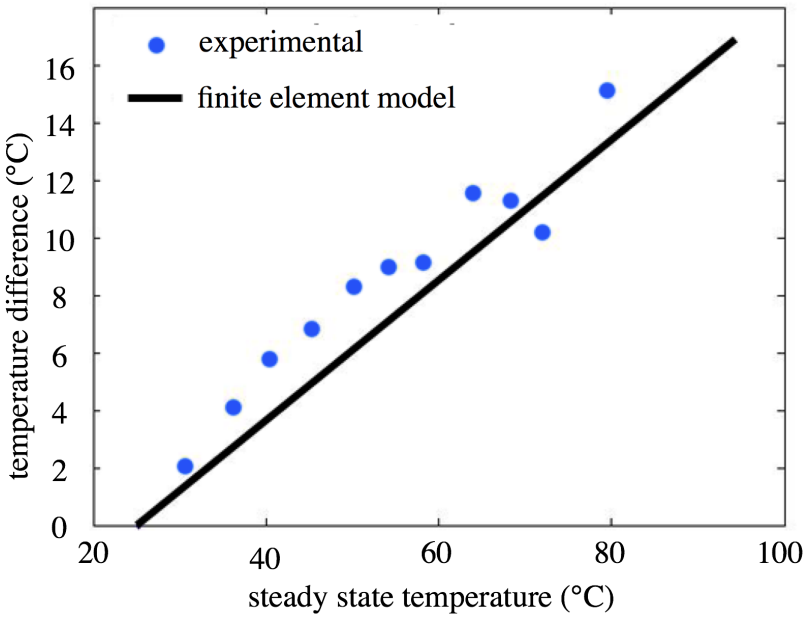

Figure 14: Experimental and finite element model analysis showing the maximum temperature difference between two 1 μL chambers positioned 1 mm apart as a function of steady state temperature of one chamber as it is irradiated.

cycles shown on the graph. It can be seen from this experiment that the shutter is able to maintain a steady state temperature, and varying the duty cycle of the signal sent to the shutter allows different temperatures to be achieved in that chamber. Furthermore, the thermal time constant of the system was measured to be 56.69 s, so operating the shutter at 10 Hz should be more than sufficient to control the temperature.

A miniature solenoid was chosen as the shutter mechanism after experimenting with other approaches. Initially, a miniature piezoelectric linear motor (SQL R3 Squiggle Motor) was used. This option had a travel distance of 6 mm, which is enough for this application. However, the speed of actuation was inadequate, and the cost is also about ten times that of the solenoid. Another option that could be used in the future is a custom liquid crystal display (LCD) based shutter. The benefit of this approach is that a custom LCD could be made into any configuration

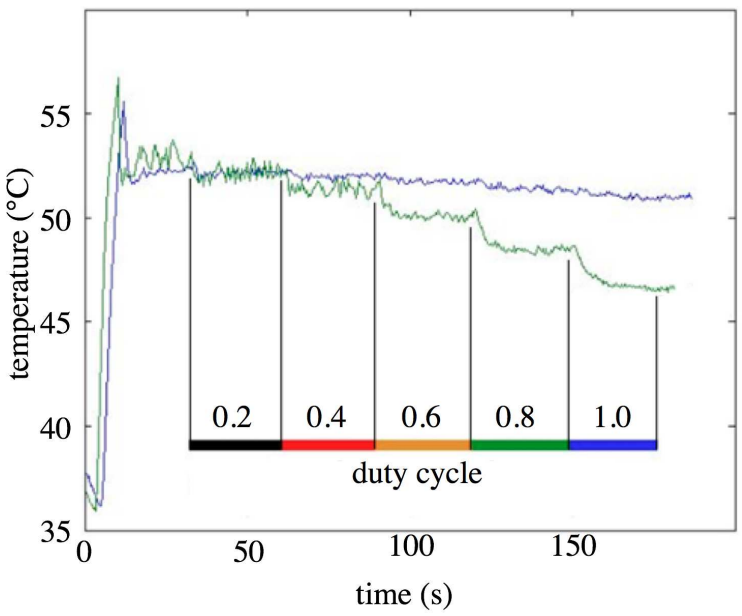

Figure 15: Temperature plots showing the ability of the shutter to decrease the steady state temperature in one chamber as a function of the duty cycle while the other chamber remains at a constant temperature.

to work with a multi-chambered chip of any geometry. However, the limitations of this technology are that a custom LCD would have to be made that would work with infrared radiation, and also a higher-powered laser would have to be used. This is due to the means by which an LCD operates. The radiation passing through the LCD is polarized so that when a voltage is applied, the liquid crystals align perpendicular to the polarized radiation, and do not let any radiation through. The theoretical maximum amount of radiation that can pass through an LCD is therefore one half of the input.

3.2 Overall System

3.2.1 Mechanical Components

The system, shown in Figure 16, consists of a single laser diode driver (Wavelength Electronics PLD5K-CH) powering two identical 1450 nm laser diodes. These are mounted on a cage rod system with the heat sink, fans, and collimating lenses on x-y

stages. The chip, as shown in Figure 17, is attached to a plate that supplies 40 psi pressure from a nitrogen tank to the inlets and outlets of both reaction chambers to prevent bubble formation. This entire assembly is then positioned on the same cage rod system for repeatable placement. The final component of the system is a shutter created from a solenoid that modulates the radiation reaching one of the reaction chambers.

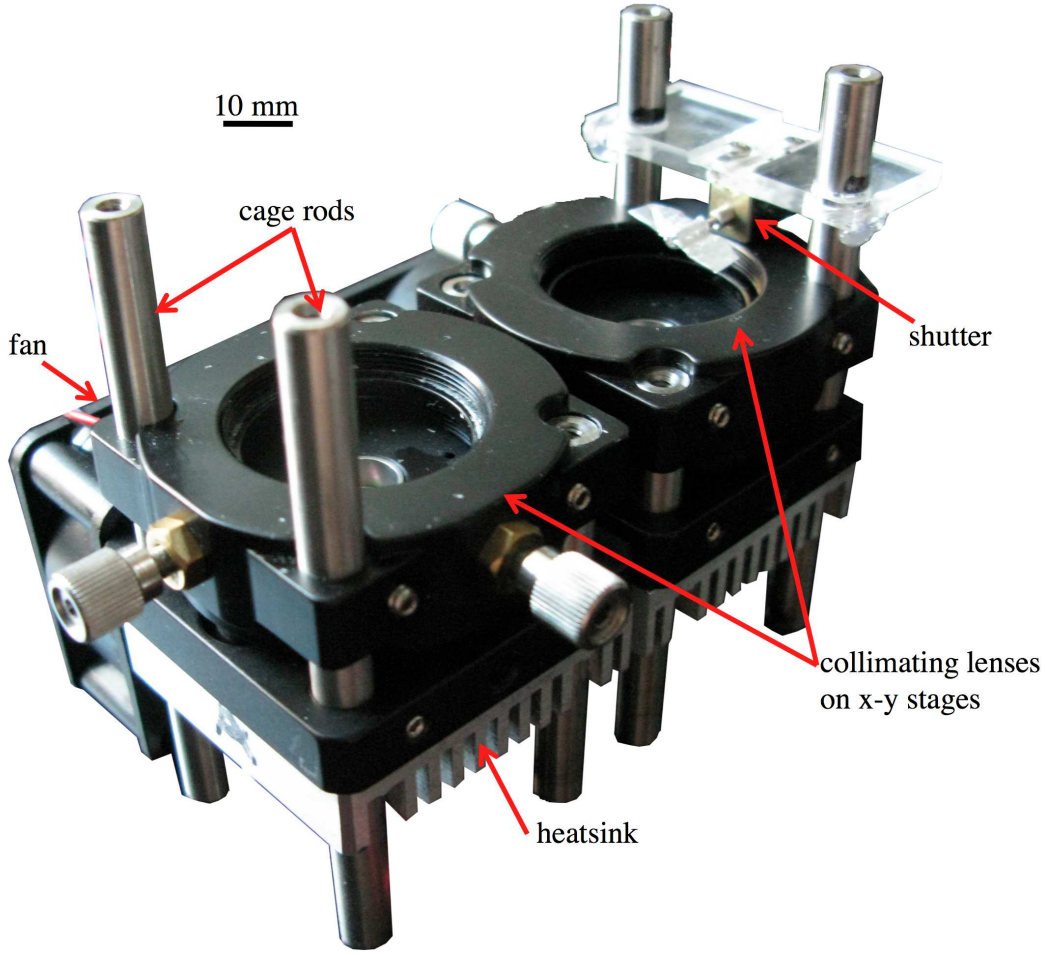

Figure 16: Infrared laser mediated PCR thermocycler with capability to perform two unique reaction simultaneously. Cage rods are used to hold the x-y stage mounted collimating lenses, shutter, and heat sink. A 0.1 ND neutral density filter is not shown.

The cage rod system allows for different components to be added, removed, and positioned easily while still being aligned with the rest of the optics. The laser diodes

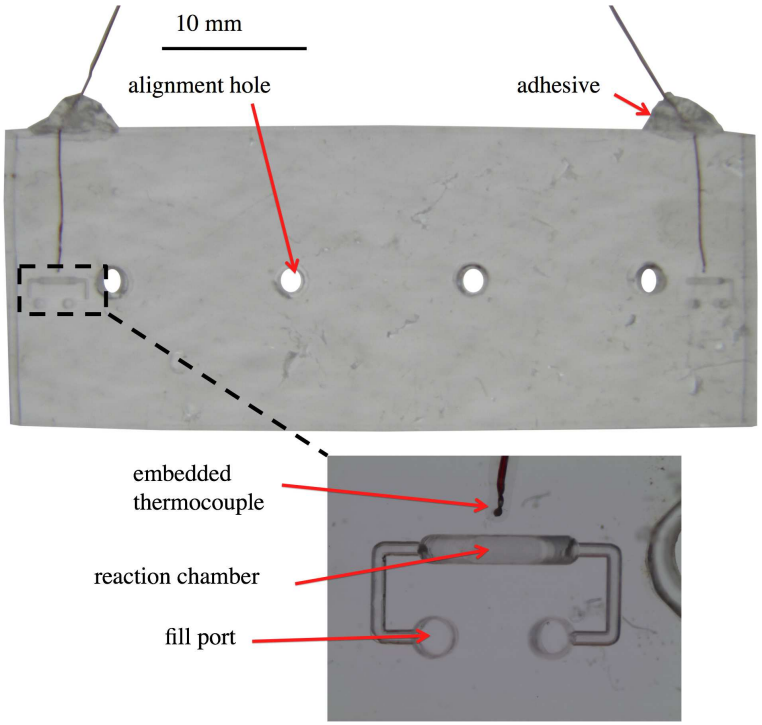

Figure 17: Two chamber PMMA chip with embedded thermocouples. Adhesive is used for strain relief of the fragile thermocouple wire. Alignment holes are used to repeatably mount the chip to the pressure plate. A pipette tip is inserted into one of the fill ports for sample filling and extraction.

are mounted on heat sinks with fans so that they stay cool and maintain a constant power output. The only components mounted on the cage rods for this system are collimating lenses and a 0.1 ND neutral density filter. The collimating lenses are focused so that the beam shape approximates the reaction chamber on the chip. Once the collimating lenses produce the correctly shaped beam, only the x-y stages are adjusted so that the beam is directly over the reaction chambers. The neutral density filter sits between the collimating lens and chip only on the laser diode that is not affected by the shutter. This prevents some of the radiation from reaching that chamber to ensure that the chamber with the shutter heats slightly faster than the one without a shutter. Faster heating for the chamber with the shutter helps both chambers run simultaneously. The chamber with the shutter has a greater change in temperature it must go through every cycle, and therefore needs slightly more power

to go through this greater temperature difference in the same amount of time.

The laser system is mounted on a PMMA base measuring 300 mm by 300 mm. The laser driver and its heat sink are also mounted on this plate. The base and pressure assembly were made on a laser cutter. After the outside of the pressure assembly was cut out, ports were drilled for the air and Luer fittings on a drill press. The Leur fitting holes were then tapped for the 10-32 threaded Leur fitting adaptor. Finally, holes were reamed in the pressure plate for a secure fit for the 1.58 mm diameter dowel pins. These pins are used for alignment for the chips to the pressure plate.

Thermocouples are embedded in the chips directly next to the reaction chambers, and are connected to the DAQ board through a thermocouple to analog voltage converter (Omega TAC80B-T) and an amplifier with a gain of 10. The thermocouple to analog converter is used to convert the signal from the thermocouples into a linear signal with an output of 1 mV/degree, and the amplifier is used because the output from the thermocouple to analog converter is only on the order of tens of mV. The laser driver is connected to a power supply and also to the same DAQ board to receive driving signals. The shutter is also connected to the DAQ board through a transistor and power supply. The transistor is used as a switch in this case because the DAQ does not have sufficient current to drive the solenoid. The DAQ board is then connected to a computer running Labview. A description of how all of the systems work together is seen in Figure 18.

This device is novel because a single laser driver is used to control the temperature in multiple chambers to achieve ideal annealing temperatures for each reaction. The solenoid based optical shutter is a simple and inexpensive way of modulating the laser radiation without the use of an independent laser driver for each laser diode. As was shown previously, a laser based infrared source is ideal for such an application

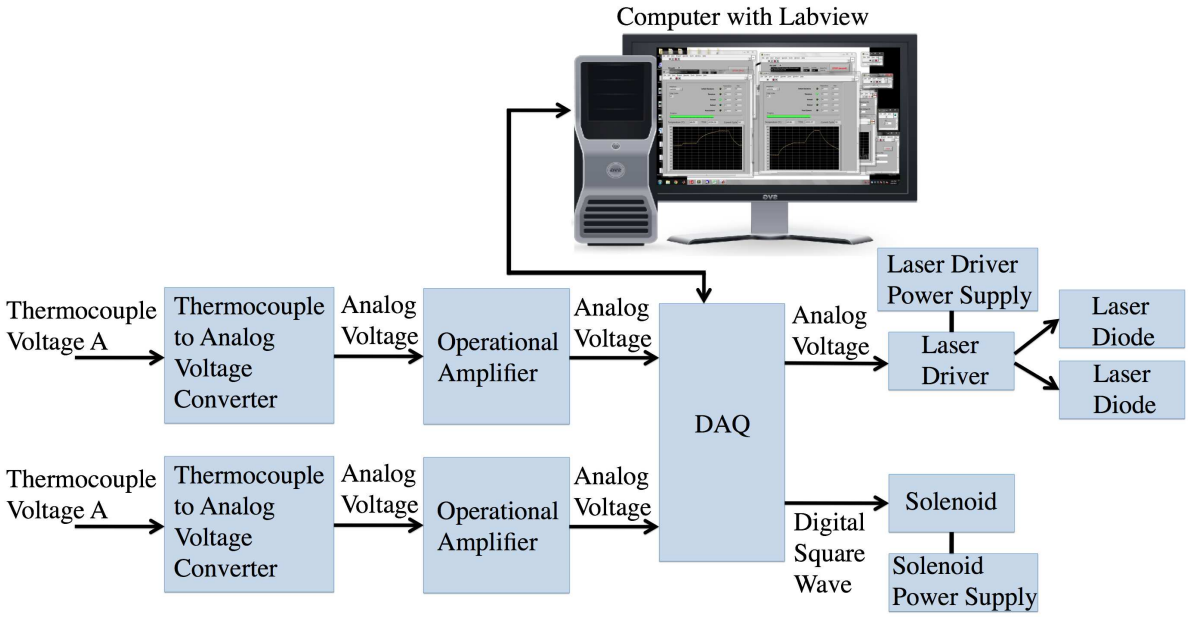

Figure 18: Diagram of the components used in a dual temperature laser-mediated PCR system. Temperature of two thermocouples is linearized by thermocouple to analog voltage converters and then amplified before being fed into a computer running Labview through a DAQ. The same Labview program outputs the necessary analog laser driving voltage and digital square wave signal needed to operate the laser driver and solenoid shutter respectively. Two identical laser diodes are connected in series to the laser driver.

because it directly heats the solution without heating the substrate. Therefore, chambers on the same chip can be packed close together and still be heated to different temperatures.

3.2.2 Pressure System

The pressure system, as seen in Figure 19, is a very important component of the device. Initial runs typically led to maximum temperatures below that of the 94°C annealing temperature, and also inconsistent temperature holds around 70°C. This was determined to be caused by air bubble formation bellow the 100°C boiling point of water. An explanation for this is that the milled surface of the chip has very small tool marks from machining, leading to air bubbles being trapped in the crevices while

filling the chip. These bubbles are not visible after filling, but expand as the solution is heated. Since the laser only heats the aqueous solution, and not the air bubbles, the temperature is inconsistent as the bubbles shift in the solution, and the overall temperature does not reach a high enough value.

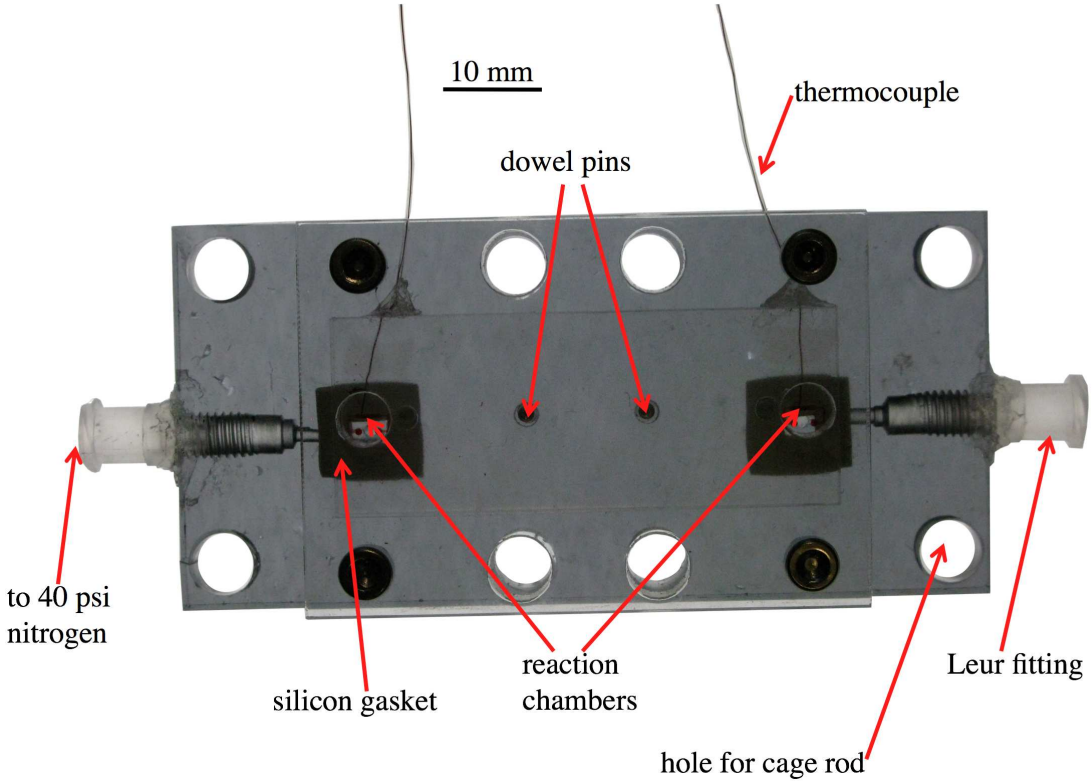

Figure 19: Dual chamber PMMA chip mounted on the pressure system with silicon gaskets. Nitrogen is used to pressurize the reaction chambers through the Leur fittings. Dowel pins are used for repeatable alignment. This entire assembly is then placed on the cage rod system.

The pressure system was developed to overcome these problems by restricting the bubbles from expanding as the solution is heated. Nitrogen is supplied at 40 psi to all four fill ports equally. A gasket is used for each chamber to prevent nitrogen from leaking. These gaskets were laser cut out of silicon and are large enough to span both fill ports on each chamber. This is necessary so that a differential pressure does not develop between the inlet and outlet of the reaction chamber and possibly evacuate

the solution from the chamber.

The chip is attached to the pressure plate by the use of a clamp that is bolted to four tapped holes on the pressure plate. There are also two 1.58 mm diameter dowel pins on the pressure plate that go through the chip and ensure that it is repeatably positioned for each run. Finally, two silicon gaskets sit between the pressure plate and the chip to ensure an airtight seal. This entire assembly is then connected to the nitrogen supply with Luer fittings and placed on the cage rod assembly.

3.2.3 Running PCR

The steps in running PCR are sample loading, attaching the chip to the pressure plate, and placing it on the cage rod assembly. Loading the sample involves pipetting PCR solution between two plugs of light mineral oil into the reaction chamber. The oil is used to passivate the surface of the chip and also to contain the solution in the path of the laser. This ensures that the entire volume of the solution receives radiation and is therefore at the same temperature, which ensures good amplifications and helps to prevent primer dimers. An image of a pipette tip with oil and solution is seen in Figure 20.

It is believed that the oil also aids with minimizing bubbles by filling the small crevices in the machined surfaces where bubbles potentially get entrapped while filling. The process for using this oil filling method is as follows: first, a 10 μL pipettor is used to collect 1.2 μL of mineral oil. Next, the pipettor is set to 2.0 μL with the oil still inside the pipette tip. This makes the oil move up the pipette tip. The pipettor is then depressed until the oil is just at the edge of the pipette tip and then the 0.8 μL of solution is collected. Finally, the pipettor is set to 3.0 μL and the same technique is used to collect the final 1.0 μL of oil. More oil is initially collected so that when the solution is flowed through the chip, there is an extra volume of oil that can be used to adjust the solution and center it within the reaction chamber. Once everything

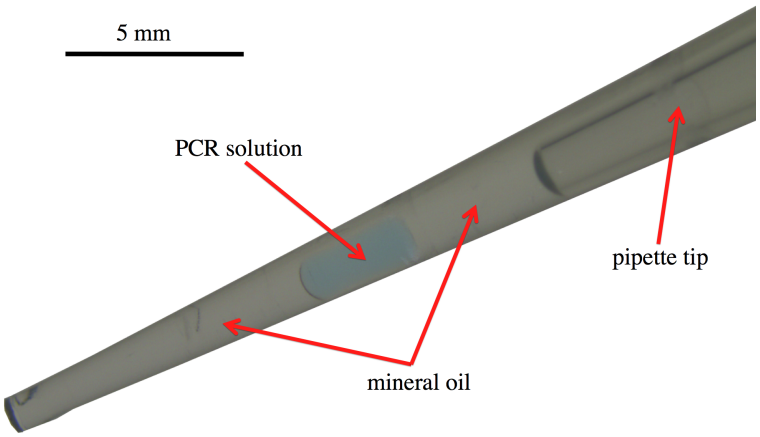

Figure 20: Photograph showing pipette tip with PCR solution resting between two plugs of oil. This is how the solution is loaded into the chip.

is loaded, the fans, laser, and solenoid power supply are turned on. Next, the user inputs the desired times and temperatures for each step of PCR, as well as the total number of cycles to run. Finally, the thermocouples are plugged into the thermocouple to analog converters and the program is initiated. After the program has finished running, the chip is taken out of the pressure plate and the sample is recovered by pipetting it out of the chip. The chip is then cleaned by first running isopropyl alcohol through the reaction chambers. Next, deionized water is run through the reaction chambers to wash away the alcohol. Finally, the same nitrogen that is used to supply pressure to the chip is used to dry off the remaining water. The chip is reused because of the thermocouples that are embedded in it, and is therefore cleaned after each run.

3.3 Temperature Measurement

Non-contact temperature measurement is a crucial requirement for PCR. Since commercially available thermocyclers are relatively slow, they have small temperature gradients. Peltier-based thermococylers take advantage of this property and embed temperature measurement devices in the plates that hold the PCR tubes. This allows

for a simple setup and fairly accurate temperature measurement, although it has been reported that temperature accuracy varies by model [32, 33].

Microfluidic systems have to use more complicated temperature measurement approaches because of the smaller scales and faster heating and cooling rates involved. Techniques used by other groups include reference chambers with thermocouples [20], fluorescent dyes [23], pyrometers [34], and resistance measurements [16]. A thermocouple directly inserted into the solution creates two problems for laser mediated PCR: reaction inhibition, and inaccurate measurements due to direct radiation of the thermocouple. Reference chambers have been used by other groups doing radiative heating based PCR in mirofluidics [20]. In this approach, a chip is made with two identical chambers position next to each other and centered over the heat source. The thermal properties of both chambers are assumed to be the same. One chamber is filled with PCR solution, while the other is filled with PCR buffer and has a thermocouple inserted that is used for temperature feedback. However, these devices use a broadband source of radiation with a large heating area. It is not possible to have a reference chamber with a laser-based system because the laser does not heat a large enough area to heat multiple chambers evenly.

3.3.1 Embedded Thermocouple Approach and Calibration

Others have used fluorescence detection with laser mediated PCR, but this requires complex calibration and the use of a fluorescence microscope for temperature feedback. Furthermore, the sensitivity of such systems decreases with increased temperature [23]. Similarly, pyrometers allow for non-contact sensing but are fairly difficult to calibrate and align [34]. Also, a pyrometer does not measure the actual solution temperature, but the surface of the microchip the solution is resting in. Calibration is necessary to relate the chip surface temperature and the internal solution temperature. Equipment for both of these non-contact temperature measurement techniques

is very expensive. The temperature measurement technique used for this device relies on a thermocouple embedded within the chip. This eliminates the problem of the thermocouple touching the solution and also the temperature inaccuracies due to direct radiation of the thermocouple by placing it away from the solution and path of the laser. Temperature measurement is done through thermocouples (Physitemp, T 240C) embedded in the chip, so that the temperature of the environment directly next to that of the heated solution is measured. Similar to the pyrometer technique, the actual temperature of the solution is not measured. To get a relationship between the chip temperature measured by the thermocouples and the actual chamber temperature, a calibration is necessary. The calibration curve relating chip temperature and solution temperature was obtained in a way similar to an open loop calibration performed for a different application [35]. First, a chip was made with thermocouples bonded in the top of the reaction chambers. The power absorbed by the aqueous solution as a function of wavelength, $P_{ABS}(\lambda)$, is calculated using the Beer-Lambert Law as $P_{ABS}(\lambda)=P_0(\lambda)(1-10^{-\alpha(\lambda)l})$, where $\alpha(\lambda)$ is the wavelength dependent absorption coefficient of water and l is the pathlength. With our wavelength and chip dimensions, the amount of radiation absorbed by the solution at the top of the chip is 90%. Therefore, placing a thermocouple here allows for a more accurate temperature measurement because it is not directly irradiated. Next, this chip was filled with a PCR buffer solution, and mounted on the device. Starting with the turn on voltage of 0.7V, the steady state temperature in each chamber was recorded up to 1.4V, which is the point where the temperature was close to that of the denaturing temperature of 94°C. This was done four times to obtain an average steady state chamber temperature as a function of laser driving voltage. Next, the actual chip used to perform PCR in was created with the aforementioned thermocouples bonded in the chip directly next to the chamber, as seen in Figure 17. As before, this chip was filled with PCR buffer and the steady state chip temperature for each chamber

was recorded as a function of laser driving voltage. This was also repeated four times to obtain the average steady state chip temperature. From these two sets of data, a correlation between chip temperature and solution temperature within the chamber was made. The calibration plot for both chambers is shown in Figure 21. The linear fit line is used in the temperature measurement program after slight adjustment to the slope. To determine the correct slope needed, a λ-phage PCR reaction was run in each chamber six times with varying slopes. The slope that gave the highest final product concentration in each chamber was then used for subsequent reactions. This temperature measurement approach is relatively simple to implement, and does not require expensive equipment. At the same time, it offers the benefit of non-contact measurement that is necessary for PCR.

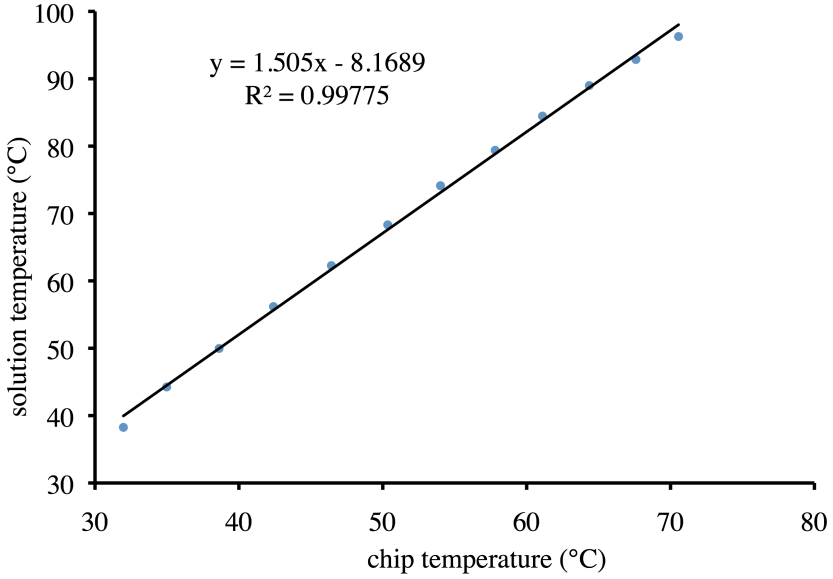

Figure 21: Temperature calibration between chip temperature measured by embedded thermocouple and solution temperature.

3.3.2 Chip Lifespan

Since it is not cost or time effective to create new chips with embedded thermocouples for each run, it is necessary to reuse chips for several PCR runs. To ensure that there

Table 2: After about 30 runs, chips have been shown to no longer be able to perform successful amplification even though heating and cooling times are maintained.

Date	Cooling Time (s)	Heating Time (s)	Final DNA Concentration (ng/μL)
5/11/12	16.76±0.445	21.14±0.656	29.33
5/11/12	17.54±1.01	20.32±0.571	23.27
5/11/12	15.94±0.699	18.32±1.00	15.89
5/11/12	15.61±0.395	15.34±0.717	0.84
5/11/12	16.42±0.208	14.10±1.04	0
5/25/12	15.20±0.607	14.90±0.276	0
5/25/12	15.50±0.632	15.50±0.718	0
5/25/12	16.24±0.671	16.60±0.303	0
5/25/12	14.58±0.643	18.72±0.492	0

is no cross contamination between runs, the chips are cleaned after each run. Cleaning involves running isopropyl alcohol and deionized water through the chambers to clean them out. Then, the chambers are dried off by flowing nitrogen through them. It was found that after repeated use, the chips tended to perform poorly, even when the same heating and cooling characteristics were observed. As seen in Table 2, using the same chip resulted in significantly different final product yields, even when the heating and cooling rates where identical. This may be due to the cleaning technique used between runs. Isopropyl alcohol is known to degrade polymers such as PMMA [36]. To counteract this problem, chips are replaced after PCR yields begin to decrease. This generally occurs after about 30 runs.

Constantly having to redo calibration curves would make this system incredibly difficult to use. It was found that only the slope of the calibration curve needed to be adjusted for new chips, and this adjustment was better guided by measuring the heating and cooling rates of the new chips. This saves time and increases the number of runs available to use per chip by eliminating calibration runs. To do this, the chip is loaded with PCR buffer and the λ-phage program is run for ten cycles. The average heating and cooling rate in both chambers is measured and compared

to heating and cooling rates that have previously been shown to successfully amplify DNA. If the rates are too fast, the slope is decreased, and if the rates are too slow, the slope is increased. Generally, an acceptable slope can be found within four runs. This drastically reduces the work and effort needed to recalibrate the temperature measurement system for each new chip.

3.4 System Control

To operate the dual temperature laser PCR system, the user inputs the desired time and temperature for each stage of PCR in the Labview front panel seen in Figure 22. This is the main Labview program that controls the subprograms and tells them what to do. The time and temperature entered by the user are used by the main program to control the laser and shutter programs based on the input from the temperature measurement program, as described in Figure 23. The front panel also displays the current cycle number, temperature, run time, and a temperature plot so the user knows that the system is working properly, and so that they are aware of when to turn the machine off and extract the sample from the chip. The front panel displayed in Figure 22 is used to control the laser driver, but a similar program is used to control the duty cycle at which the shutter is operated. The front panel of that program looks identical to the one shown here, and it operates almost identically, except for the fact that it controls the shutter and not the laser driver.

The Labview program operates as follows: first, the temperature of each thermocouple is read and translated to a chamber temperature with the equation obtained from the calibration curve. Next, the program determines which stage of PCR it is currently in (initial denaturing, denaturing, annealing, extension, or final extension), and compares the desired temperature at that stage with the measured temperature. A proportional-derivative (PD) controller is used to modify the analog laser driving voltage so that the error between the desired and measured temperature is

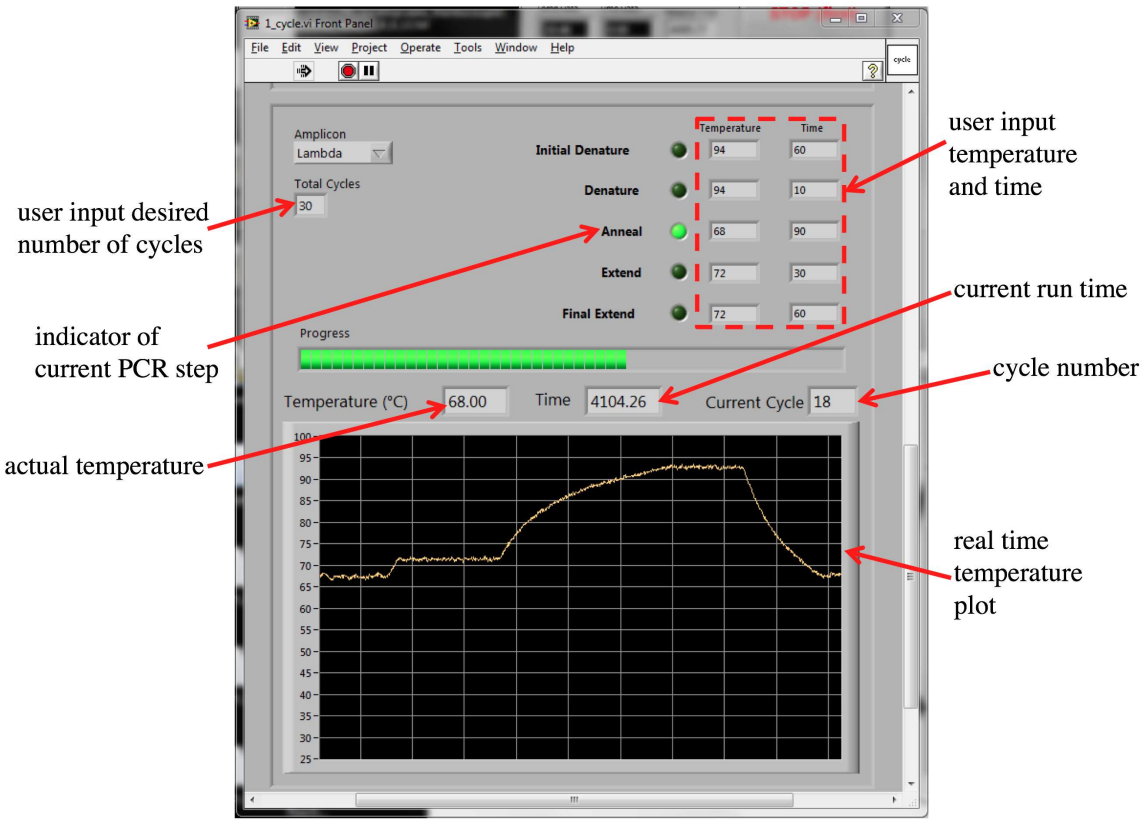

Figure 22: Front panel of the main program showing the user input times, temperatures, and number of cycles to run for one of the chambers. This also displays the run time, current cycle number, current temperature, a real time temperature plot of the thermal cycling, and the current stage of PCR. An identical front panel is used to control the time and temperature of the other chamber.

minimized, and also so that over and undershoot when transitioning between holding temperatures are minimized. The laser driver is controlled with an analog signal because this allows for finer resolution of laser driving voltage, and therefore a smoother temperature profile, than a digital pulse width modulation signal.

While holding the temperature of the solution in the chamber at the desired value, the program waits the amount of time input by the user before moving on to the next stage. If the next stage is at a higher temperature, the laser is turned on to its maximum driving voltage. If the next stage is at a cooler temperature, the laser is shut off and the solution is allowed to cool through natural convection. When

the desired temperature is reached, the PD controller is turned on again and the temperature value is maintained for the input time. This process is repeated for each stage of PCR for the desired number of PCR cycles. The final task carried out by the program is saving a file of the time, temperature, and laser driving voltage. Similarly to how the laser driver voltage is changed based on the desired temperature through a PD controller, another PD controller is used to change the duty cycle of the pulse width modulation signal sent to the shutter to vary the amount of time the shutter is open and closed. The shutter operates at 10 Hz and has a travel distance of 8.9 mm. The chambers are spaced 40 mm apart and are therefore thermally independent. The maximum temperature difference between the two chambers can be greater than 30°C, allowing for optimized annealing temperatures of any two PCR reaction. The entire Labview program consists of a single temperature measurement program, a program that drives the laser, a program that drives the shutter, and two virtually identical sets of main programs that carry out the PCR cycles. These sets of programs determine what stage of PCR it is currently in, and what inputs to send to the laser. Also, this is where the user inputs the desired times, temperatures, and number of cycles. A breakdown of how all the programs work in unison can be seen in Figure 23.

A feature that was added to the main program of the shutter after initial testing was an automatic override at the denaturing step. Sometimes, the chamber affected by the shutter lags behind the other chamber because it has a greater temperature difference it must go through. The neutral density filter helps reduce some of this lag by decreasing the power to the non-shutter chamber, but sometimes the two chambers still do not synchronize. Therefore, if the non-shutter chamber reaches denaturing first, the program assumes that both chambers have reached denaturing. If this happens, the program realizes that the shutter chamber is lagging and immediately blocks all the radiation to that chamber so that it can get to the annealing stage

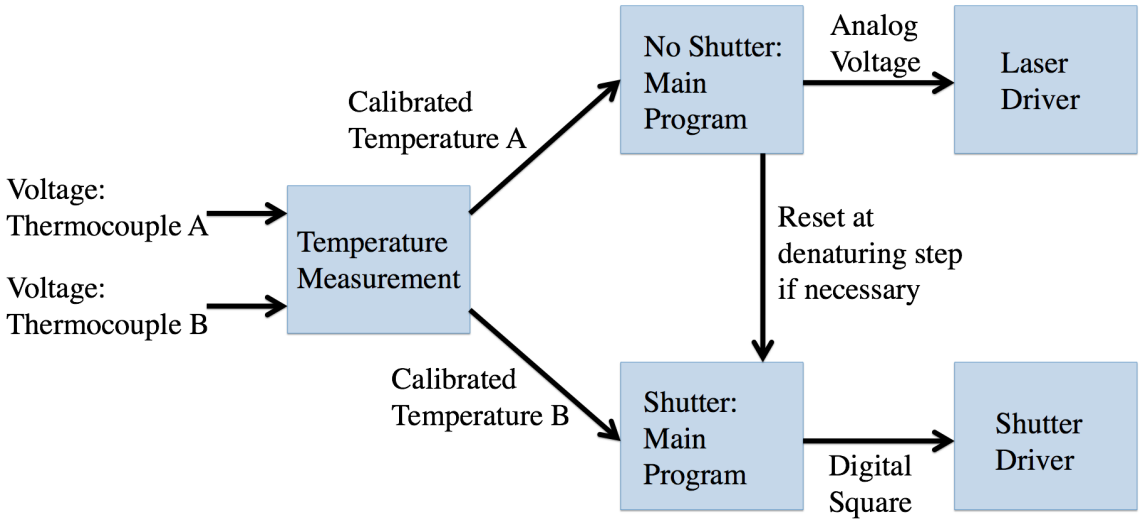

Figure 23: Operation procedure for Labview programs for performing PCR in two chambers. The temperature measurement program reads both thermocouple values and uses the calibration equation to output those values to the two main programs. The main programs determine which step of PCR is currently being performed and adjust the temperature as necessary by sending an analog voltage to the laser driver program, and a digital square wave PWM signal to the shutter driver program.

faster and not lag on the next cycle. This built in override can be seen in Figure 24. This feature keeps both programs synchronized since the cycle number is increased every time the program reaches the denaturing temperature, so it is impossible for one chamber to finish before the other. If the shutter chamber reaches denaturing first, there is no problem with synchronization because the laser will stay on until the other chamber reaches denaturing. While this probably affects PCR efficiency in the shutter chamber since a few cycles may be skipped, it is very useful for keeping the program running smoothly. Also, PCR is typically done for enough cycles that skipping a few will not affect the amplification.

While the laser diodes can be driven at a maximum of 2.7V to achieve a laser power of 710 mW, they are only operated up to 1.9V, which results in 470 mW of power. This is done so that the solution heats up slowly enough to ensure an accurate temperature measurement from the thermocouples embedded in the chip.

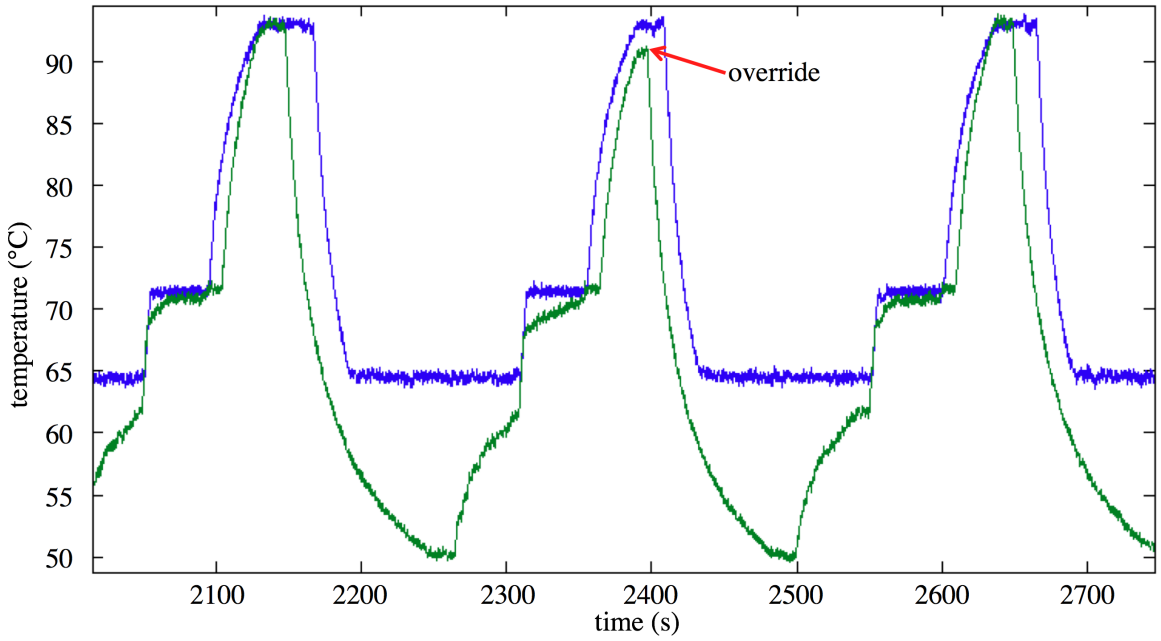

Figure 24: Override at denaturing step if the shutter affected chamber does not reach denaturing first. The temperature in this chamber immediately goes down if denaturing is reached in the other chamber first. This data was taken from an actual successful amplification run.

While this does reduce overall cycling time, it ensures proper amplification with the chosen temperature measurement method.

3.5 Device Validation

To demonstrate the capabilities of this device, two different PCR reactions were prepared and ran simultaneously on the same chip. The first was an amplification of the 500 base pair λ-phage DNA with a 65°C annealing temperature. This is a reaction done by many other groups as a means of verifying successful amplification [20]. The other was an amplification of the 600 base pair EpsteinBarr virus (EBV) with a 50°C annealing temperature. This virus was obtained from a collaboration with the Center for Disease Control and Prevention. It is part of the herpes family, and one of the most common viruses in humans.

A pre-mix tube (Bioneer Accupower PCR Premix) was used for both reactions to save time. This tube contains the buffer, $MgCl_2$, DNA polymerase, and nucleotides so that the only ingredient the user needs to add are water, primers, and the DNA template. The preparation of the λ-phage reaction is as follows: 29 μL of molecular biology grade water were added to the premix tube, vortexed, and spun down. To this, 15 μL of BSA (1 mg/mL), 1 μL of forward and reverse primers (20 μM), and 5 μL of DNA (45.8 μg/mL) were added. This 50 μL volume was split into 10 equal volumes of 5 μL each for ease of use and so samples were not contaminated every run. BSA was added because it has previously been shown to aid microchip PCR [37]. The primer sequences used were 5'-GATGAGTTCGTGTTCGTACAACTGG-3' for the forward primer and 5'-GGTTATCGAAATCAGCCACAGCGCC-3' for the reverse primer.The preparation of the EBV mixture is as follows: 43 μL of molecular biology grade water were added to the premix tube, vortexed, and spun down. To this, 1 μL each of forward and reverse primers (50 μM) were added. From this 45 μL, volumes of 1 μL were taken and added with 1 μL of DNA ($1.25\text{x}10^{-3}$ ng/μL). These samples were loaded into the chip with oil plugs as previously described. The EBV reaction was loaded into the chamber affected by the shutter, since it has a lower annealing temperature, while the λ-phage reaction was loaded into the other chamber. The simultaneous temperature plots of both chambers can be seen in Figure 25, with a closeup shown in Figure 26. The total run time was slightly less than two hours. While this is slow compared to other microfluidic thermocyclers, there are several reasons for this. First, this is not an optimized run; the hold times were kept conservative to ensure amplification and most likely can be decreased. Also, since it was important to show the ability to amplify two reactions with very different temperatures, the EBV reaction was chosen. This reaction has a very low annealing temperature and therefore takes a long time to cool. There is no active cooling on this system, so this added feature on future designs would be of great benefit in reducing

the run time.

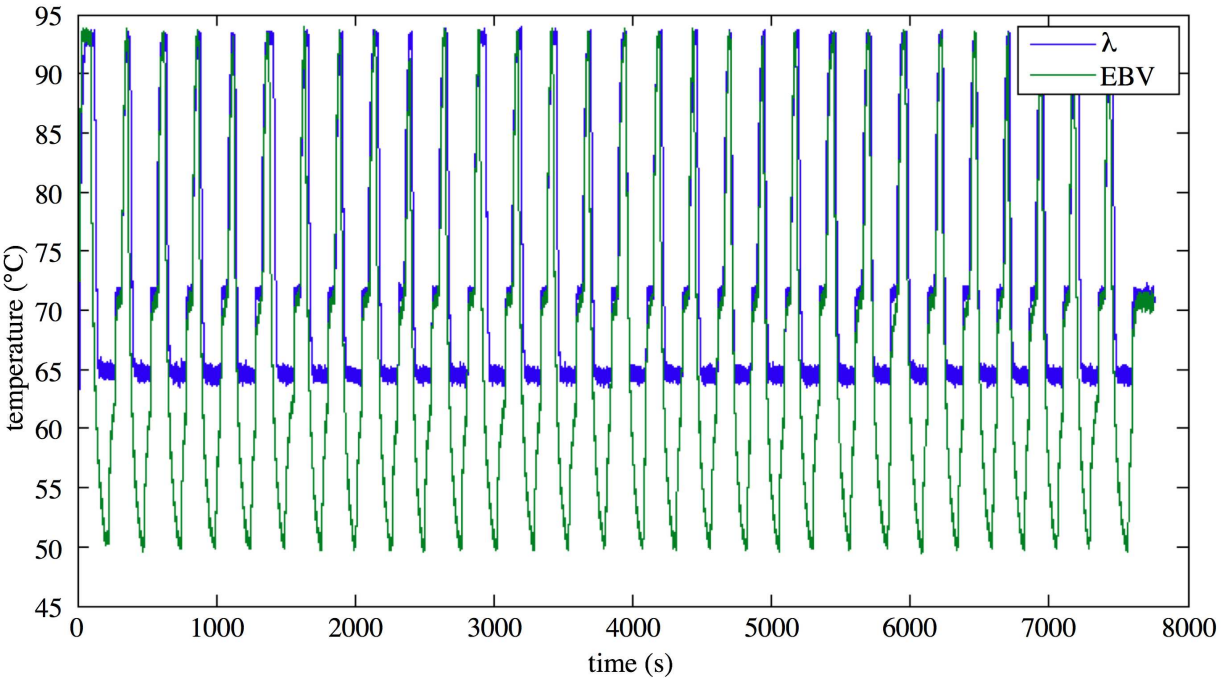

Figure 25: Full 30 cycle temperature profile for two chamber PCR for targets having an annealing temperature difference of 15°C.

Electrophoretic detection of the final concentration of PCR products was performed on an Agilent Bioanalyzer. This was done for both the samples run on this device, and for the positive controls. The positive controls are 5 μL reactions taken from the same master mix used for the microfluidic reactions and run on a conventional thermocycler (Biorad MJ Mini). The electropherograms for the λ-phage and EBV reactions run on the chip can be seen in Figures 27 and 28 respectively. For comparison, the run times for the EBV and λ-phage reactions on this thermocycler were 2 hours and 1.5 hours respectively.

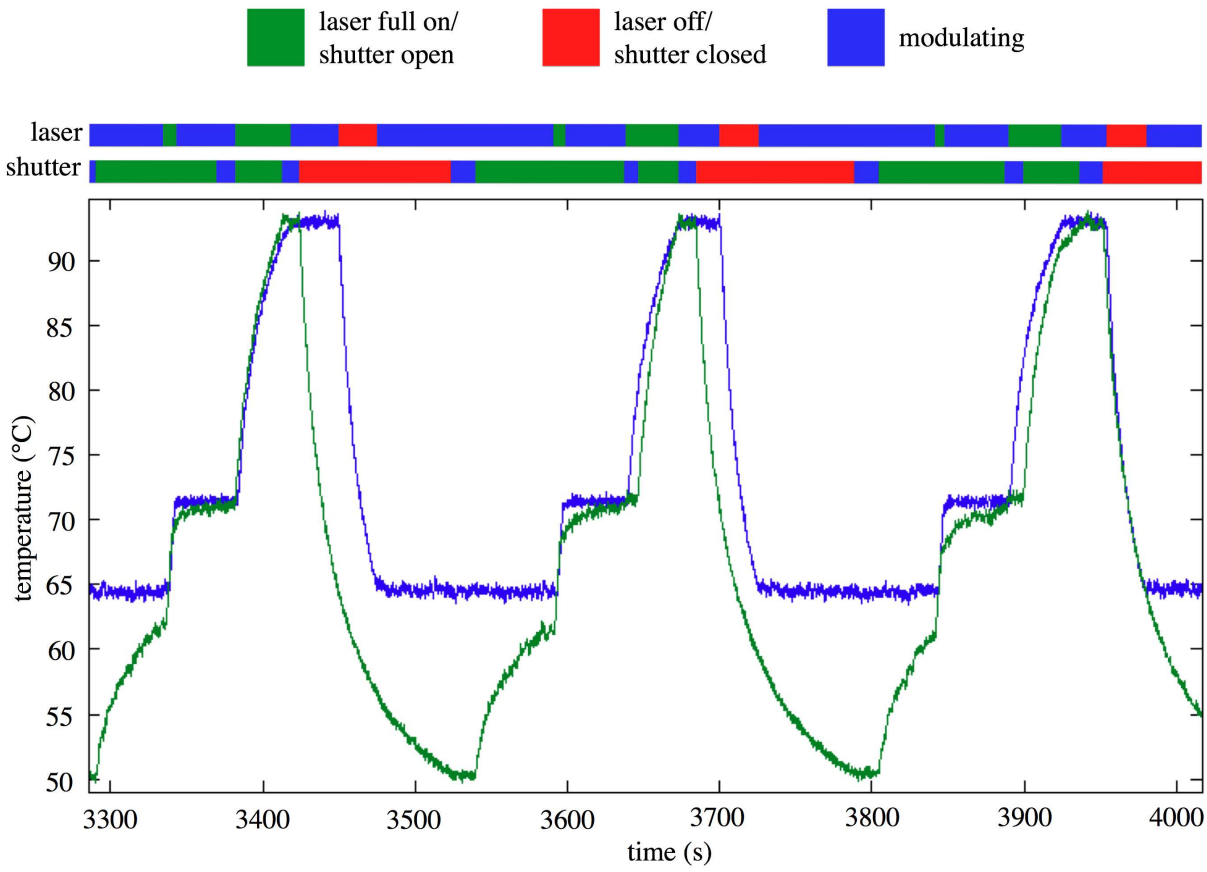

Figure 26: Closeup of temperature profile in two chambers showing large annealing temperature difference. Bars at the top of the graph show how the laser and shutter were being operated at every point in time.

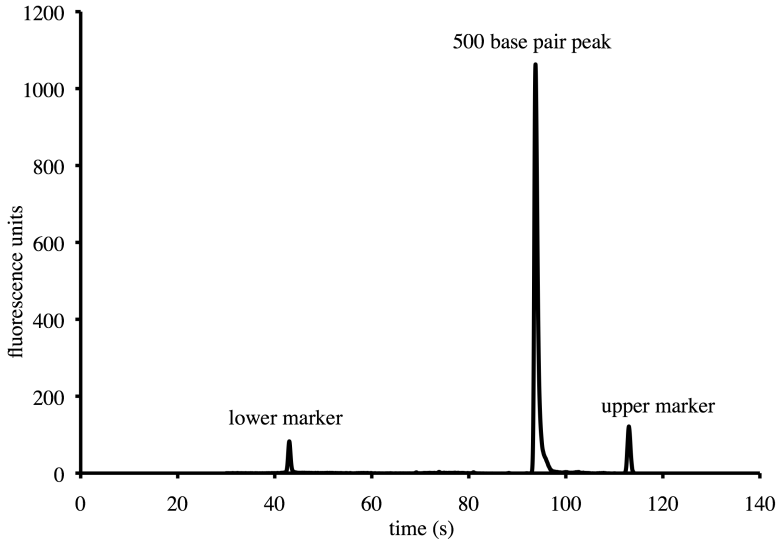

Figure 27: Electropherogram of λ-phage reaction performed simultaneously as EBV reaction on the same device showing 500 base pair peak.

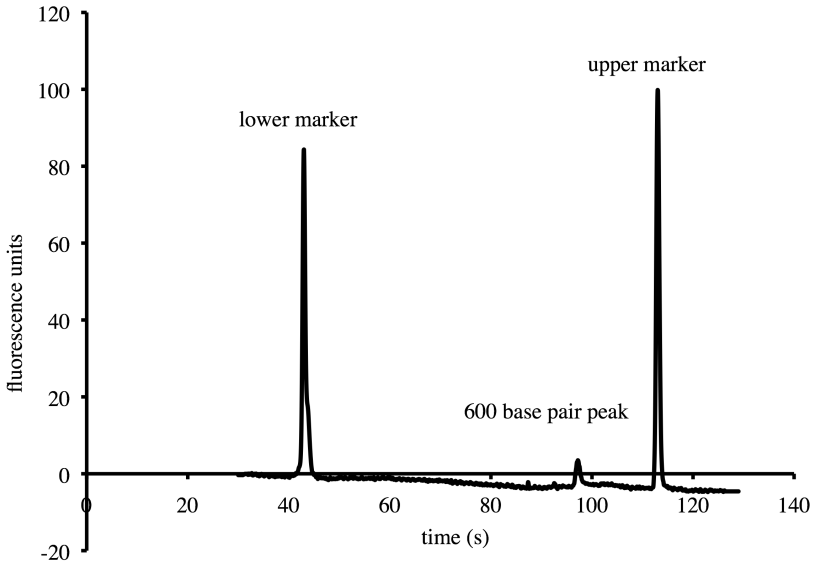

Figure 28: Electropherogram EBV of reaction performed simultaneously as λ-phage reaction on the same device showing 600 base pair peak.

CHAPTER IV

CONCLUSION

Microfluidic PCR has built upon the "gold standard" of virus detection with work on decreasing the time and cost associated with traditional PCR while also including capabilities for upstream and downstream processing. The device built here has further built upon microfluidic PCR by introducing a system that can amplify DNA targets with arbitrary annealing temperatures simultaneously on the same device. A laser based approach is used because the monochromatic source allows for heating of only the solution, and not the surrounding substrate. This, and the fact that the laser radiation is focused allows for two distinct temperatures to be achieved on the same device. Since the two laser diodes in this system are driven identically by the same laser driver, a shutter was developed that modulates the radiation reaching one of the chambers. The shutter has been shown to effectively control the temperature in that chamber by varying the duty cycle at which it is driven. This system further relies on a microfluidic polymer chip with embedded thermocouples for closed loop temperature feedback. This allows for accurate, simple, non-contact temperature measurement. The system has been shown to work successfully by the amplification of λ-phage DNA and EBV DNA simultaneously on the same chip.

4.1 Future Work

The system presented here is a proof of concept device that demonstrates the capabilities of laser-based infrared mediated thermocycling for PCR. While it is a good first effort, many components and procedures can be improved for the next version. The main focus points would be the elimination of thermocouples, the integration of a more powerful laser, and the scale up of this concept. While the polymer chips used

in this device are simple and inexpensive to manufacture, the embedded thermocouples lead to a chip that is not completely disposable. For this work, the chips were reused until they began to show decreased amplification. At this point, the thermocouples were removed and reused in new chips. This is impractical in a real world environment, and a completely disposable chip is ideal. Work has already been done to incorporate a thermal camera into the system as the temperature measurement device. The advantages of the thermal camera are that it is completely non-contact, the camera is detached from the chip, and it is easily scalable to many temperature measurements with the same device. A Labview program has already been made that incorporates the thermal camera as the temperature measurement device and it is capable of running PCR exactly the same as the device presented here. The camera was not used here because it does not measure the temperature of the solution, but rather the temperature at the surface of the chip. However, as shown here, a calibration can be done that relates the solution temperature to the chip surface temperature, similarly to how the embedded thermocouple only measures the temperature of the chip immediately next to the reaction chamber. With repeatable placement of the chip and a securely fixed camera, this method will be very similar to that of the embedded thermocouples used on this proof of concept device. An initial goal of this project was to utilize a single laser diode in combination with a lens array to simultaneously heat two reaction chambers with one laser. However, as mentioned previously this was not possible because commercially available laser diodes do not have sufficient power to heat two chambers in such a manner. A custom made 16 fiber laser has been purchased that outputs 1 watt of power per fiber. This device can be driven identically to the system presented here, and will allow for a scale up of the number of reactions on a chip. The shutter system will also have to be scaled up, and the advantage of using solenoid based shutter as shown here is their low price, fast shutter frequency, and easy integration. While two reactions on the same chip is

a big milestone in microfluidic PCR technology, it is only a proof of concept of what laser-based thermocyclers can achieve. The temperature measurement scheme, microfluidic chips, and optical shutter based modulation from this device are all scalable to many more chambers.

REFERENCES

[1] K. Mullis, F. Faltoona, S. Scharf, R. Saiki, G. Horn, H. Erlich, "Specific enzymatic amplification of DNA in vitro: the polymerase chain reaction," *Cold Spring Harbor Symp Quant Biol*, **51**, pp. 263 - 273, 1986.

[2] L.J.R. van Elden, M.G.J. van Kraaij, M. Nijhuis, K.A.W. Hendriksen, Ad W. Dekker, M. Rozenberg-Arska, A. M. van Loon, "Polymerase chain reaction is more sensitive than viral culture and antigen testing for the detection of respiratory viruses in adults with hematological cancer and pneumonia," *Clinical Infectious Diseases*, **34**(2), 177-183, 2002.

[3] A. Virolainen, P. Salo, J. Jero, P. Karma, J. Eskola, M. Leinonen, "Comparison of PCR assay with bacterial culture for detecting Streptococcus pneumoniae in middle ear fluid of children with acute otitis media," *J. Clin. Microbiol.* **32**(11):2667, 1994.

[4] W. Rychlik, W.J. Spencer, R.E. Rhoads, "Optimization of the annealing temperature for DNA amplification in vitro," *Nucleic Acids Research*, **18**(21), pp. 6409-5412, 1990.

[5] R.S. Cha, W.G. Thilly, "Specificity, efficiency, and fidelity of PCR," *Genome Research*, **3**, pp. 18-29, 1993.

[6] C. T. Wittwer, K.M. Ririe , R.V. Andrew, D.A. David, R.A. Gundry, U.J. Balis, "The LightCycler(TM) a microvolume multisample fluorimeter with rapid temperature control," *Biotechniques*, **22**, pp. 176-181, 1997.

[7] R. Higuchi, C. Fockler, G. Dollinger, R. Watson, "Kinetic PCR analysis: real-time monitoring of DNA amplification reactions," *Biotechnology*, **11**, pp. 1026-1030, 1993.

[8] C.T. Wittwer, D.J. Garling, "Rapid cycle DNA amplification: time and temperature optimization," *Biotechniques*, **10**, pp. 76-83, 1991.

[9] J.G. Lee , K.H. Cheong , N. Huh , S. Kim , J.W. Choi, C. Ko, "Microchip-based one step DNA extraction and real-time PCR in one chamber for rapid pathogen identification," *Lab Chip*, **6**, pp. 886-895, 2006.

[10] U. Lehmann, C. Vandevyver, V.K. Parashar, M.A.M. Gijs, "Droplet-based DNA purification in a magnetic lab-on-a-chip," *Angewandte Chemie*, **45**(19), pp. 3062-3067, 2006.

[11] R.H. Liu, J. Yang, R. Lenigk, J. Bonanno, P. Grodzinski, "Self-contained, fully integrated biochip for sample preparation, polymerase chain reaction amplification, and DNA microarray detection," *Anal. Chem.*, **76**(7), pp. 1824-1831, 2004.

[12] A.T. Woolley, D. Hadley, P. Landre, A.J. deMello, R.A. Mathies, M.A. Northrup, "Functional integration of PCR amplification and capillary electrophoresis in a microfabricated DNA analysis device," *Anal. Chem.*, **68**(23), pp. 4081-4086, 1996.

[13] E.T. Lagally , C.A. Emrich, R.A. Mathies, "Fully integrated PCR-capillary electrophoresis microsystem for DNA analysis," *Lab Chip*, **1**, pp. 102-107, 2001.

[14] F.C. Huang, C.S. Liao, G.B. Lee, "An integrated microfluidic chip for DNA/RNA amplification, electrophoresis separation and on-line optical detection," *Electrophoresis*, **27**, pp. 3297-3305, 2006.

[15] M.U. Kopp, A.J. de Mello, A. Manz, "Chemical amplification: continuous-flow PCR on a chip," *Science*, **280**(5366), pp. 1046-1048, 1998.

[16] C.S. Liao, G.B. Lee, H.S. Liu, T.M. Hsieh, C.H. Luo, "Miniature RT-PCR system for diagnosis of RNAbased viruses," *Nucleic Acids Research*, **33**(18), p. e156, 2005.

[17] N. Agrawal, Y.A. Hassan, V.M. Ugaz, "A pocket-sized convective PCR thermocycler," *Angewandte Chemie*, **46**(23) pp. 4316-4319, 2007.

[18] E. K. Wheeler, W. Benett, P. Stratton, J. Richards, A. Chen, A. Christian, K.D. Ness, J. Ortega, L.G. Li, T.H. Weisgraber, K. Goodson, F. Milanovich, "Convectively driven polymerase chain reaction thermal cycler," *Anal. Chem.*, **76**(14), pp. 4011-4016, 2004

[19] C.J. Easley, J.M. Karlinsey, J.M. Bienvenue, L.A. Legendre, M.G. Roper, S.H. Feldman, J.P. Landers, "A fully integrated microfluidic genetic analysis system with sample-in-answer-out capability," *Proceedings of the National Academy of Sciences*, **103**(51), pp. 1972-1977, 2006.

[20] A.F.R. Hühmer, J.P. Landers, "Noncontact infrared-mediated thermocycling for effective polymerase chain reaction amplification of DNA in nanoliter volumes," *Anal. Chem.*, **72**(21), pp. 5507-5512, 2000.

[21] R.P. Oda, M.A. Strausbauch, A.F.R. Hühmer, N. Borson, S.R. Jurrens, J. Craighead, et al, "Infrared mediated thermocycling for ultrafast polymerase chain reaction amplification of DNA," *Anal. Chem.*, **70**(20), pp. 4361-4368, 1998.

[22] B.C. Giordano, J. Ferrance, S. Swedberg, A.F.R. Hühmer, J.P. Landers, "Polymerase chain reaction in polymeric microchips: DNA amplification in less than 240 seconds," *Anal. Biochem.*, **291**, pp. 124-132, 2001.

[23] M. Slyandev, Y. Tanaka, M. Tokeshi, T. Kitamori, "Photothermal temperature control of a chemical reaction on a microchip using an infrared diode laser," *Anal. Chem.*, **73**, pp. 4037-4044, 2001.

[24] H. Kim, S. Vishniakou, G.W. Faris, "Petri dish PCR: laser-heated reactions in nanoliter droplet array," *Lab Chip.*, **9**(9), pp. 1230-1235, 2009.

[25] H. Terazono, A. Hattori, H. Takei, K. Takeda, K. Yasuda, "Development of 1480 nm photothermal highspeed real-time polymerase chain reaction system for rapid nucleotide recognition," *Jpn. J. Appl. Phys.*, **47**, pp. 5212, 2008.

[26] J.S. Chamberlain, R.A. Gibbs, J.E. Rainer, P.N. Nguyen, C. Thomas, "Deletion screening of the Duchenne muscular dystrophy locus via multiplex DNA amplification," *Nucleic Acids Research*, **16**(23), pp. 11141-11156, 1988.

[27] O. Henegariu, N.A. Heerema, S.R. Dlouhy, G.H. Vance, P.H. Vogt, "Multiplex PCR: critical parameters and step-by-step protocol," *BioTechniques*, **23**, pp. 504-511, 1997.

[28] T.M. Rose, E.R. Schultz, J.G. Henikoff, S. Pietrokovski, C.M. McCallum, S. Henikoff, "Consensus-degenerate hybrid oligonucleotide primers for amplification of distantly related sequences," *Nucleic Acids Research*, **26**(7), pp. 1628-1635, 1998.

[29] R.T. Kelly, A.T. Woolley, "Thermal bonding of polymeric capillary electrophoresis microdevices in water," *Anal. Chem.*, **75**(8), pp. 19411945, 2003.

[30] A.A. Sodemann, J.R. Mayor, "Parametric investigation of precision in tool-workpiece conductivity touch-off method in micromilling," *Transactions of the North American Manufacturing Research Institution of SME*, **37**, pp. 565-572, 2009.

[31] D.S. Lee, S.H. Park, H. Yang, K.H. Chung, T.H. Yoon, S.J. Kim, K. Kim, Y.T. Kim, "Bulk-micromachined submicroliter-volume PCR chip with very rapid thermal response and low power consumption," *Lab Chip*, **4**, pp. 401-407, 2004.

[32] I. Yang, Y.H. Kim, J.Y. Byun, S.R. Park, "Use of multiplex polymerase chain reactions to indicate the accuracy of the annealing temperature of thermal cycling," *Anal. Biochem.*, **338**, pp. 192-200, 2005.

[33] Y.H. Kim, I. Yang, Y.S. Bae, S.R. Park, "Performance evaluation of thermal cyclers for PCR in a rapid cycling condition" *BioTechniques*, **44**, pp. 495-505, 2008.

[34] M.G. Roper, C.J. Easley, L.A. Legendre, J.P. Landers, "Infrared temperature control system for a completely noncontact polymerase chain reaction in microfluidic chips," *Anal. Chem.*, **79**(4), pp. 1294-1300, 2007.

[35] N. Pak, D.C. Saunders, C.R. Phaneuf, C.R. Forest, "Plug-and-play infrared laser-mediated PCR in a microfluidic chip," *Biomedical Microdevices*, **14**(2), pp. 427-433, 2012.

[36] E.H. Andrews, L. Bevan, "Mechanics and mechanism of environmental crazing in a polymeric glass," *Polymer*, **13**(7), pp. 337-346, 1971.

[37] C. Zhang, J. Xu, W. Ma,W. Zheng, "PCR microfluidic devices for DNA amplification," *Biotechnology Advances*, **24**(3), pp. 243-284, 2006.